



**Michigan
Technological
University**

Michigan Technological University
Digital Commons @ Michigan Tech

Dissertations, Master's Theses and Master's Reports

2021

DEVELOPMENT AND VALIDATION OF DYNAMIC PROGRAMMING ALGORITHM FOR ECO APPROACH AND DEPARTURE

Vasu Goyal

Michigan Technological University, vasug@mtu.edu

Copyright 2021 Vasu Goyal

Recommended Citation

Goyal, Vasu, "DEVELOPMENT AND VALIDATION OF DYNAMIC PROGRAMMING ALGORITHM FOR ECO APPROACH AND DEPARTURE", Open Access Master's Thesis, Michigan Technological University, 2021.
<https://doi.org/10.37099/mtu.dc.etr/1314>

Follow this and additional works at: <https://digitalcommons.mtu.edu/etr>



Part of the [Navigation, Guidance, Control, and Dynamics Commons](#)

DEVELOPMENT AND VALIDATION OF DYNAMIC PROGRAMMING
ALGORITHM FOR ECO APPROACH AND DEPARTURE

By

Vasu Goyal

A THESIS

Submitted in partial fulfillment of the requirements for the degree of

MASTER OF SCIENCE

In Mechanical Engineering

MICHIGAN TECHNOLOGICAL UNIVERSITY

2021

© 2021 Vasu Goyal

This thesis has been approved in partial fulfillment of the requirements for the Degree of MASTER OF SCIENCE in Mechanical Engineering.

Department of Mechanical Engineering – Engineering Mechanics

Thesis Co-Advisor: *Dr. Jeffrey D. Naber*

Thesis Co-Advisor: *Dr. Darrell Robinette*

Committee Member: *Dr. Ahammad Basha Dudekula.*

Department Chair: *Dr. William W. Predebon*

Table of Contents

List of Figures.....	vi
Acknowledgments	x
List of Abbreviations	xii
Abstract.....	xiii
1 Introduction.....	1
1.1 Connected and Automated Vehicle Technologies - Background	1
1.2 Research goals and objectives.....	2
1.3 Thesis Layout	5
2 Eco Approach and Departure.....	6
2.1 Intelligent Signalized Intersections	7
2.2 Relevant research outside MTU.....	8
2.3 Relevant research at MTU	11
3 Research environment	15
3.1 Vehicles under consideration	15
3.1.1 Chevrolet Volt – Gen 2.....	15
3.1.2 Chevrolet Bolt – 2019.....	16
3.1.3 Vehicle Instrumentation.....	18
3.2 Data collection	20

3.2.1	On-road data collection	20
3.2.1.1	MTU drive cycle.....	20
3.2.1.2	RSU loop	22
3.2.2	Track data collection	26
4	Model Development	28
4.1	Dynamic programming and its components	28
4.1.1	Inputs to DP	29
4.1.2	Cost function	31
4.1.3	Constraints to DP.....	33
4.1.4	Simulation Results for GM-Volt Gen II.....	35
4.2	Baseline model development	37
4.3	Bolt- Eco-AnD Algorithm Development.....	43
4.3.1	Reduced-order energy model development process.....	43
4.3.1.1	Step 1: Understanding the data.....	44
4.3.1.2	Step 2: Understanding the powertrain efficiencies....	45
4.3.1.3	Step 3: Developing the response surface from the dynamometer data.	46
4.3.1.4	Step 4: Validating the developed response surfaces..	47
4.3.2	Brake Blending strategy	49
4.3.3	Developing Eco-AnD model for Bolt.....	55
4.3.3.1	Cost function	55
4.3.3.2	Constraints and inputs to DP	55

4.3.4	Simulation Results for Bolt	56
5	Results and Discussions.....	59
5.1	Eco-AnD energy benefits – Volt.....	59
5.1.1	Simulations	59
5.1.2	On-road Comparison	61
5.1.3	Track testing	66
5.2	Eco-AnD energy benefits – Bolt	72
5.2.1	Simulations	72
5.2.2	On-road comparison	74
5.2.3	Computation Time	75
5.2.4	Variable Approach Distance.....	77
5.2.5	Variable Vehicle Mass.....	79
6	Conclusions and future work	82
6.1	Conclusion.....	82
6.2	Future Work	83
7	Appendix.....	85
7.1	SPaT and MAP message directory.....	85
7.2	Computation Time	85
	Reference List.....	87

List of Figures

Figure 1 Illustration of DSRC communication between vehicle and signalized intersection	6
Figure 2 Current phase illustration	7
Figure 3 GM-Volt Gen II	16
Figure 4 GM-Bolt 2019	17
Figure 5 Vehicle Instrumentation in boot.....	18
Figure 6 Laptop connected to vehicle performing real-time vehicular control.....	19
Figure 7 MTU Drive cycle, original image taken from Google maps.	21
Figure 8 RSU loop, original image taken from Google maps.	23
Figure 9 RSU loop Intersection Grade	26
Figure 10 ACM Intersection Map	27
Figure 11 Distance from intersection description	28
Figure 12 Pictorial view of inputs to DP	29
Figure 13 Schematic for calculation cost function - Volt.....	31
Figure 14 Pictorial representation of passing window calculation.....	35
Figure 15 Simulation result for 6x6 intersection.....	37
Figure 16 EPA drive cycles speed vs acceleration scatter plot	39

Figure 17 6x6 intersection baseline comparison - Volt.....	41
Figure 18 Dynamometer drive cycle with EPA drive cycles	44
Figure 19 Dynamometer drive cycle with aggressive acceleration and braking.....	45
Figure 20 Bolt reduced-order energy model result.....	48
Figure 21 Drive cycle for brake blending analysis.....	50
Figure 22 BF analysis	52
Figure 23 0-150 Nm total brake torque zoomed-in plot.....	54
Figure 24 Simulation result for Bolt.....	57
Figure 25 6x6 intersection baseline comparison - Bolt	58
Figure 26 RSU loop simulation energy analysis	63
Figure 27 RSU loop energy savings with respect to the number of intersections with complete stops	65
Figure 28 MTUDC Energy Savings vs Intersections with complete stops	66
Figure 29 Location-based speed profile tracking.	69
Figure 30 Schematic for determining speed request based on the reference point.	70
Figure 31 Track-testing result for 6x6 intersection	71
Figure 32 MTUDC Energy Savings vs Intersections with complete stops – Bolt	75
Figure 33 Iteration of different approach distance	79
Figure 34 Iteration of different mass	81

List of Tables

Table 1 Literature review comparison table.....	13
Table 2 Vehicle comparison table	17
Table 3 Vehicle Instrumentation details.....	19
Table 4 MTU drive cycle comparison with EPA standard drive cycles	22
Table 5 RSU loop intersection details	24
Table 6 RSU loop intersection elevation details	25
Table 7 ACM Intersection details.....	27
Table 8 Summary of inputs to DP	29
Table 9 Discretization of inputs to DP	30
Table 10 Constraints to DP.....	33
Table 11 Passing window timing calculations.	34
Table 12 6x6 intersection physical scenario.....	35
Table 13 EPA drive cycles avg acceleration and deacceleration	39
Table 14 Bolt Motor torque regions	46
Table 15 Bolt Power coefficients for energy model.....	47
Table 16 Bolt- Dynamometer energy prediction results	48
Table 17 Eco-AnD simulated results for RSU loop intersections.....	60

Table 18 Eco-AnD simulated results for ACM intersections - Volt	61
Table 19 Eco-AnD on-road testing results for RSU loop.....	63
Table 20 6x6 Intersection details.....	67
Table 21 Source of inputs to DP for track testing	68
Table 22 Track testing summary	72
Table 23 Eco-AnD results for RSU loop intersections - Bolt	73
Table 24 Eco-AnD results for ACM intersections – Bolt.....	74
Table 25 Computation time for different grid discretization	76
Table 26 Computation time for different control input limits	77
Table 27 Effect of different approach distance.....	78
Table 28 Effect of different mass	80
Table 29 V2I message directory	85
Table 30 Computation time for different grid discretization (full table).....	85

Acknowledgments

This research traces the most important part of my academic journey, which was a steep learning curve for me in many ways. The road to the success of this research was full of challenges and new learnings. It would not have been possible to bring this research to a conclusion without the admirable support that I have received throughout my journey.

I am deeply grateful to Dr. Jeffery D Naber, who allowed me to work on this esteemed project. Thank you for having an unwavering belief in me. He has been an ideal mentor and under his brilliant supervision, I have learned a lot. He has always encouraged my ideas and provided me with the utmost freedom to exercise them. I owe a sincere thank you to Dr. Darrell Robinette for being an excellent co-advisor and helping me resolve the toughest of problems. His insightful comments and invaluable suggestions have helped me shape this research so well.

A special thanks to Dr. Ahammad Basha Dudekula. Not just my mentor at MTU, he has been more like an elder brother to me. He has always shown me the right direction and guided me in the best way possible. Additionally, I thank all my colleagues at APS labs who provided me with all the assistance and support whenever needed. I would like to thank all my friends at MTU who motivated me constantly throughout my master's studies.

And last but not the least, I want to thank my parents and my sister, to whom I owe my life. I will forever be indebted to them for believing in me and helping me in

accomplishing all my achievements. During my journey, their love and support meant the world to me.

This work was supported by the following funding: Advanced Research Projects Agency-Energy (ARPA-E), a subunit of the U.S. Department of Energy under award number DE-AR0000788, and The American Center for Mobility through U.S. Department of Energy award number DE-EE0008407.

This is contribution No. 5 of the Advanced Power Systems Research Center, at Michigan Technological University.

List of Abbreviations

Eco-AnD – Eco approach and departure

CAV – Connected automated vehicles

V2I – Vehicle to infrastructure

V2V – Vehicle to vehicle

SpaT – Signal phase and timing

ACM – American Center of Mobility

DOE – Department of Energy

MTU – Michigan Technological University

DSRC – Dedicated short-range communication

DP – Dynamic Programming

BEV – Battery electric vehicle

BSM – Basic safety messages

SAE – Society of Automotive engineers

Abstract

Eco Approach and Departure (Eco-AnD) is a Connected and Automated Vehicle (CAV) technology developed to reduce energy for crossing a signalized intersection or set of intersections in a corridor that features vehicle to infrastructure (V2I) communication capability. Eco-AnD technology uses the information of the signal phase and timings (SPaT) received from the V2I communication to optimize the vehicle's speed profile and produce an energy-efficient maneuver to cross the intersection.

The energy-reduction potential of the Eco-AnD is examined by developing baseline models that represent real-life human driver behaviors. The developed baseline models were validated for a corridor comprised of six intersections around a real-world drive cycle (MTU Drive Cycle) to verify average energy prediction accuracy of about 95 %.

The Eco-AnD algorithm is devised for two vehicles (GM-Volt Gen II & GM-Bolt), both with different powertrain architectures but capable of working in electric-only mode. In simulations, the developed algorithm showed an energy-saving potential of 70-90 kJ per intersection around the corridor of the MTU drive cycle for both vehicles. For the RSU loop (a subset of MTU drive cycle) up to 8 % of energy reduction is observed. Vehicle level testing of the optimized speed profiles was carried out at the American Center of Mobility (ACM) on GM-Volt Gen II to demonstrate an energy-saving of 40-50 kJ per intersection on real road conditions.

1 Introduction

1.1 Connected and Automated Vehicle Technologies - Background

As it is a widely known notion that access to sufficient information about a problem leads to better decision making. A Connected Automated Vehicle (CAV) works on a similar principle and possesses the capability of receiving and using information from various sources in the surroundings to improve driving in terms of energy, time, and safety. In the work by Islam, et al. [1], the communications with surroundings are classified as V2I, V2V, V2C, V2P, V2X where V stands for a vehicle, I stands for infrastructure, C stands for cloud, P stands for pedestrian and X stands for anything in surrounding capable of communicating. From the information broadcasted by these sources, intelligent vehicle controllers can be developed to make the vehicle's motion safe and efficient.

Extensive research focus has been conducted on CAV technologies in the last decade. The U.S. Department of Energy (DOE) has played a key role in the advancement of these technologies by supporting multiple projects. The ARPA-E NEXTCAR (Next-generation energy technologies for connected and automated on-road vehicles) was launched by DOE ARPA-E to develop 20-30 % energy savings by use of CAV technologies [2]. To bring this project to fruition, DOE created a team of several institutions including General Motors (GM), Michigan Technological University (MTU), Pennsylvania State University (Penn State), Purdue University, Southwest

Research Institute (SwRI), The Ohio State University, University of California (Berkeley), University of California (Riverside), University of Delaware, University of Michigan, and the University of Minnesota.

As a part of the NEXTCAR project, MTU and GM partnered to develop advanced CAV technologies including eco-routing, speed harmonization, in-situ vehicle parameter characterization, cooperative driving between multiple vehicles, intelligent PHEV mode blending, and eco approach and departure. Details of each technology and its energy benefits can be found in [3]. The aim was to develop, validate and demonstrate these technologies for a fleet of eight GM-Volt Gen II and show a cumulative energy-saving of 20 % and an increased range of 6 %. MTU team has demonstrated the energy-saving capabilities of individual technologies as well as with the combination of them to meet the NEXTCAR's objectives. These energy-saving demonstrations were conducted around the Michigan Technological University including a loop of five signalized intersections.

1.2 Research goals and objectives

This research expands the work done at MTU by Brandon Narodzonek on developing Eco Approach and departure algorithm for PHEV (Chevrolet Volt Gen II) [4]. In that study, a dynamic programming (DP) based algorithm was developed for six different intersections around the MTU drive cycle corridor and the energy reduction benefits of the algorithm were determined by comparing the simulation results to human driver maneuvers. On an experimental level, 2-4 % of energy savings around the MTU drive

cycle were demonstrated by providing the driver/vehicle with prior knowledge of traffic light phase timings. A detailed explanation of his work has been presented in section 2.3.

The goals of this research are to expand the existing work on Eco Approach and Departure algorithm developed by Narodzonek. The research begins by continuing the development of an existing dynamic programming-based algorithm and validating the optimized speed profiles at simulation as well as at the vehicular level. In addition, the focus is placed on developing baseline speed profiles for the various intersections around the MTU drive cycle to compare and therefore prove the energy-saving potential of the developed Eco-AnD algorithm. The validity of baseline speed profiles was checked by comparing the energy consumption against on-road human driver maneuvers at the intersections. Further, to extend the scope of the Eco-AnD algorithm, a similar algorithm was developed for the fully electric vehicle, the GM-Bolt.

Several objectives were identified and achieved during the progression of research to meet the research goal. The primary objectives of this research are:

1. Extend the existing dynamic programming algorithm to generate the optimized speed profiles for all possible traffic light phase scenarios by introducing additional constraints on DP.
2. Develop baseline speed profiles to simulate normal and aggressive human driving behaviors and perform the energy consumption comparison between optimized and baseline driving scenarios. This will provide the basis for the

determination of energy savings by the devised Eco-AnD algorithm in simulations before experimenting on roads and proving grounds.

3. Perform the on-road data collection to calibrate the baseline human driver models for the intersections around a corridor of the MTU drive cycle and ACM proving grounds.
4. Perform the on-road and closed-course track testing of the optimized speed profiles to demonstrate the energy savings by the optimized speed profiles against human driving under given similar conditions.
5. Design and develop a reduced-order energy model for the fully electric vehicle (BEV - GM Bolt), that can be used in determining the energy consumption by the cost function of DP. As a part of this, the brake blending strategy for the vehicle is to be determined to account for the distribution of braking torque between friction brake and regenerative braking.

While developing the Eco-AnD algorithm several assumptions were made. It was assumed that the information required from the DSRC communication such as phase timings, cycle timing, current phase information, and intersection location was available 300 m before the intersection. Then it is assumed that there is a 300 m of departure distance available for the vehicle post crossing the intersection. For simplicity, it is assumed that there was no traffic while approaching the intersection and the signal phase timings/durations were certain and deterministic.

1.3 Thesis Layout

This thesis is organized as follows. Chapter 2 describes what Eco-AnD is and the state of the art. A detailed literature review is presented to show the relevant work that has been accomplished outside MTU and explains the potential room for advancements. Details of relevant research conducted at MTU have been laid out explaining the published results and Narodzonek's research. Chapter 3 of the thesis describes the details of the research environment explaining the vehicles used for research, the drive cycles for on-road testing, and intersections at the American Center of Mobility (ACM) proving grounds used for data collection. In chapter 4, details of the model development and been laid out for both the vehicles under consideration for this research. Chapter 5 focuses on the validation results for both the baseline human driver model and the optimized speed profiles. Lastly, Chapter 6 provides a summary and conclusion from the work along with potential future work.

2 Eco Approach and Departure

Eco approach and departure is a CAV technology that lets the vehicle cross the signalized intersection efficiently both in terms of energy and time. The aim is to provide the vehicle controller the information via V2I communication that is necessary for generating an optimized velocity profile. The communication from the intersection contains information such as time to next phase, current phase, GPS coordinates of intersection and some intersection can also broadcast the information about speed advisory that can aid vehicle controllers. An illustration of the vehicle to infrastructure communication is shown in Figure 1. The vehicle controller uses the information from the V2I communication and develops the speed profile such that the intersection is crossed during the green phase while running at the optimal point of the propulsion system.

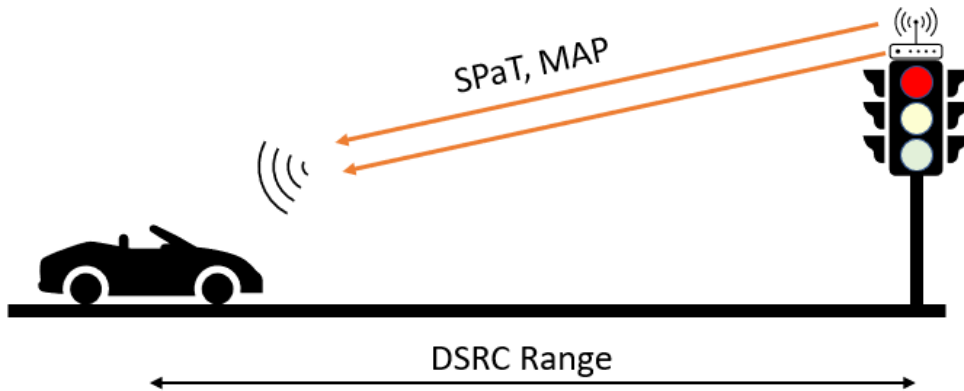


Figure 1 Illustration of DSRC communication between vehicle and signalized intersection

2.1 Intelligent Signalized Intersections

Intelligent signalized intersections refer to those intersections that can broadcast various intersection-related information via the DSRC [5]. DSRC has a typical range of about 250-300 m and can go up to 1000 m, so a vehicle with the capability of communicating with the infrastructure can receive the information from an intersection considerable distance behind the intersection giving a sufficient window for the vehicle controller to compute an optimal trajectory and then follow it to cross the intersection efficiently. DSRC follows the SAE J2735 standard [6]. It consists of various messages that can be used for V2X communication but a signalized intersection broadcasts only SPaT and MAP messages. SPaT messages consist of information about signal phase and timing. Information like the current phase, time to next phase, and cycle times are broadcasted by the intersection.



Figure 2 Current phase illustration

Figure 2 illustrates the current signal in the traffic light. From left to right on the figure, we can see the current phase to be green, yellow, and red. According to SAE J2735, the signal states are assigned numbers for ease of understanding. The green phase is assigned 5, the yellow phase is assigned 7, and the red phase is assigned 3. Time to

next signal is the time remaining for the current phase state at the moment when the message is broadcasted. MAP messages consist of geological information about the intersection like intersection GPS coordinates, speed limits on various movement states of intersection.

2.2 Relevant research outside MTU

Extensive research has been conducted on developing Eco-AnD algorithms in the last decade around the world. Various methods have been considered while designing algorithms that can be made the vehicle cross the intersection without coming to a complete stop. From the various research conducted, some of the key works are described below.

1) One example is the work done by Asadi and Vahidi [7]. They developed the velocity optimization technique by considering the information available from traffic lights about the current signal and time to the next signal. They developed two-stage algorithms to solve this problem. The first stage was a rule-based algorithm to find the optimal speed profile to cross the intersection safely and the second stage was making the vehicle follow the optimized speed by using an MPC controller. Their study was done in simulations, and it showed a 59 % fuel saving capability and 17.5 % range increase for 9 km distance with 9 signalized intersections. The research uses the Powertrain Systems Analysis Toolkit (PSAT) developed by Argonne National Laboratory to evaluate the energy-saving and fuel economy of the vehicle. Although the rule-based algorithm is a powerful tool to generate an optimized speed profile, it

does not consider the vehicle's powertrain efficiency maps and road elevation profiles while optimizing the speed profile. Including these factors can further improve the fuel economy of the vehicle while crossing the intersection.

2) Vögele and Endisch [8] developed a dynamic programming-based algorithm to generate velocity profiles for Eco-AnD. This study aimed to develop a plethora of optimized speed profiles considering the traffic and driver behavior and then give out one best possible speed profile suitable for the current situations. The algorithms consider the weighing factors between the traffic ahead and the driver comfort to select the velocity profile. Also, the study suggests that reducing the travel time (time to cross the intersection) can reduce fuel consumption, but a quantifiable measure of energy-saving is not mentioned. There are several dynamic programming algorithms discussed in the paper to find out most time economic algorithm. Discretization of velocity and distance is made much coarse to save computation time but this has its disadvantages. Considering the DSRC range of 300 m, the discrete level of 50 m may create problems when implemented on real vehicles. Having only 6-speed points in the speed profile may lead to abrupt acceleration which may be uncomfortable to passengers and may not be very fuel-efficient.

3) Guo, et al. [9], have attempted to solve the problem for a parallel hybrid vehicle by developing a bi-level MPC controller. The problem is divided into two loops, the outer loop is optimizing the vehicle's velocity by communicating with the infrastructure whereas the inner loop is keeping the vehicle parameters such as torque split ratio and gear shift schedule at optimum level. The study suggests by developing a two-layered

algorithm can make the optimization problem computationally efficient by a factor of nearly 310 for velocity optimization and by 279 for torque split and gear schedule optimization. These results are based upon the simulation carried out in AMESim. Although the developed algorithm shows good energy-saving potential in simulations, it may be difficult to implement a bi-level MPC controller in real-time considering the computation power required for solving the complex problem of 2 stage optimization.

4) Hao, et al. [10], have developed an Eco-AnD algorithm for adaptive traffic lights which change signal phase and timings considering the traffic situation at the corridor. Their work aimed at implementing the algorithm for the real-world case and they developed a speed advisory system for the driver considering the traffic around the Eigen vehicle and the traffic light signal phase and timings. Their algorithm was able to demonstrate an energy-saving of 6 % on real road conditions and 2 % on energy-saving on the overall drive cycle. As an innovative idea it is, it has its limitation. With the driver speed advisory system, the driver always must keep an eye on the instrumentation cluster to follow the speed which is both not safe and will have an error in maintaining the actual optimal speed.

5) HIL testing of the Eco-AnD algorithm was done in one of the studies done by Cantas, et al. [11]. Their algorithm uses a method called green wave state selector which uses one out of four pre-defined criteria to alter the vehicle speed. The inputs to the algorithm are the vehicle state, SPaT information, and distance, and based upon the four states it outputs a speed change command. The states tell whether to accelerate, decelerate, maintain the speed, or come to a complete stop. Using this algorithm,

they were able to demonstrate a fuel consumption reduction of 3 % and 7 % improvement for the multiple intersection model. The green wave algorithm has the limitation of considering the vehicle's propulsion system efficiency maps and road elevation changes into considerations.

6) Sun, et al. [12], dealt with the problem of uncertainty in the phase timings of the adaptive traffic lights. The algorithm that is developed is bolstered by the traffic data collected over the years and then analyzed. The most likely phase timings according to the time of the day are analyzed and then used for speed planning for a CAV. Once the uncertainty in the phase timing is dealt with, the problem of generating the optimized speed profile is solved by using the distance-based dynamic programming algorithm. In simulations, their study shows the potential of saving 40% fuel as compared to the human driver model. The determination of the traffic light phase is based on data collected. This type of solution may fall apart for the newly installed traffic lights which lack historical data to develop the data-driven optimization technique.

2.3 Relevant research at MTU

The first research work related to Eco-AnD was done by Biswajit Barik in his Master's thesis which was published in 2017, [13]. The work focused on developing the CAV technologies by using sequential quadratic programming (SQP) tools to optimize the vehicle's speed profile. The algorithm could simulate the Eco-AnD for three consecutive signalized intersections and simulated an energy savings of 8-9 % for GM-Volt Gen II.

As a part of ARPA-E NEXTCAR, MTU has developed a study on Eco Approach and departure. The study has focused on demonstrating the potential energy savings on a multi-model plug-in hybrid vehicle – Chevy Volt Gen II over the RSU loop. On the simulation level, the study showed a potential of 13-44 % energy-saving per intersection whereas the experimental trials showed a potential of 25-35 % energy-saving. Similar analysis showed an energy savings of about 4 % on the overall MTU drive cycle.

Another study at MTU was conducted by Narodzonek in his dissertation focused towards developing the dynamic programming-based velocity optimization technique that would take the information from the vehicle’s CAN channel and SPaT & MAP information from DSRC and give the output of an energy-efficient speed profile. The algorithm runs using the ‘dpm’ function to solve the backward dynamic programming problem.

In his study, the vehicle of prime focus was Chevrolet Volt Gen II and only the CD mode operation of the vehicle was considered. To calculate the energy consumption as a part of the cost function of dynamic programming, a reduced-order energy model was used. The details of this model can be found in [14]. The equation for the CD mode energy model can be written down as one shown in (1). The DP uses the reduced-order energy model as the cost function while assuming an additional constant auxiliary load of 1.5 kW, which gives the cost function as (2).

$$E = C_1 + C_2T + C_3v + C_4Tv + C_5T^2 + C_6v^2 \quad (1)$$

$$C = E \cdot dt + 1.5 \cdot dt \quad (2)$$

The constraints to the DP are defined such that the vehicle maintains the road speed limit and crosses the intersection only within the green phase. The algorithm relies on the information on SPaT and MAP broadcasted from the DSRC at the intersection to perform the speed optimization. In his research work, the energy-saving potential of Eco-AnD at the RSU loop is 5 %, increasing the MPGe of the vehicle by 8.1%. For the MTU drive cycle, the energy savings range from 1.8 to 4 % that accounts for an increase in MPGe by 1.9 %.

To make one on one comparison with all the relevant research work, a comparison table is developed, Table 1. The table covers various properties of the Eco-AnD algorithm that certain studies may or may not consider while developing the research. This table covers the literature review from research conducted both outside and at MTU. At the end of the table, the scope of this research work is also laid out to compare the characteristics of this research in comparison to the literature review above.

Table 1 Literature review comparison table

Research	Optimization Technique	Vehicle Propulsion system dynamics	Road dynamics consideration	Simulation/High IL/On- road/Track Testing	Traffic consideration	Adaptive Traffic lights
-----------------	-----------------------------------	---	--	--	----------------------------------	--

Clemson University	Rule-based algorithm	X	X	Simulation	X	X
THI, Germany	DP	Y	X	Simulation	Y	X
Jilin University, China	MPC	Y	X	Simulation	X	X
U of C, Riverside	State selection algorithm	X	X	On-road	Y	Y
OSU	Green wave	X	X	HIL	X	X
U of C, Berkely	DP	Y	X	Simulation	X	Y
Barik, MTU	SQP	X	Y	Simulation	X	X
Narodzoni, MTU	DP	Y	Y	Simulation/On-road testing	X	X
Goyal, MTU	DP	Y	Y	Simulation/On-road testing/Track Testing	X	X

3 Research environment

For any study, the research environment plays a very important role in achieving goals. Due to abundant resources available at MTU, it was possible to bring this research to success. This research focuses on two vehicles with different powertrain architectures for developing the optimization algorithm. A Chevrolet Volt – Gen II (Compound split – PHEV) and a Chevrolet Bolt (EV). Details of these vehicles are presented in Section 3.1.1 and 3.1.2 respectively. Then section 3.1.3 gives the details of the vehicle instrumentation that was used to carry out the vehicle level testing of the optimized speed profiles. The drive cycles used for this research study are discussed in section 3.2 and detailed information on the intersections encountered on these drive cycles is laid out. Details of track testing at ACM proving grounds are also provided in this section.

3.1 Vehicles under consideration

3.1.1 Chevrolet Volt – Gen 2

Chevrolet Volt – Gen 2 is a light-duty multi-mode plug-in hybrid vehicle. Broadly characterizing, the vehicle can operate in two different modes depending upon the vehicle's high voltage battery's state of charge. Charge depleting (CD) mode is the pure electric operation of the vehicle's powertrain. In this mode, the only propulsion source is the high voltage battery, and the engine is shut off making the vehicle's operation analogous to any fully electric vehicle. The charge sustaining (CS) mode of the vehicle is the hybrid operation of the vehicle where the engine and two motor/generator units of the vehicle propel the vehicle. For the following research

application, much focus has been devoted to the CD mode of the vehicle. The vehicle has an all-electric range of 53 miles when fully charged [15].



Figure 3 GM-Volt Gen II

3.1.2 Chevrolet Bolt – 2019

Chevrolet Bolt 2019 is a pure electric vehicle with a rechargeable energy storage system of 60kWhr capacity. The vehicle is propelled by a single traction motor of 200 HP driving the front wheels. The vehicle has a driving range of 238 miles on a full charge and a maximum speed of 91 MPH [16].



Figure 4 GM-Bolt 2019

Table 2 Vehicle comparison table

Vehicle Characteristic	Chevrolet Volt Gen II	Chevrolet Bolt
Powertrain Architecture	PHEV with dual-motor power split.	EV with single final drive ratio
Modes of operation	Charge depleting (CD) & Charge sustaining (CS)	Charge depleting (CD)
Curb Weight (kg)	1607.0	1616.0
F0 (N)	172.2	126.3
F1 (N/mps)	4.5	2.0
F2 (N/mpss)	0.2	0.4
Maximum all electric range (mi)	53.0	238.0

3.1.3 Vehicle Instrumentation

The vehicles used in this research were part of DOE ARPA-E NEXTCAR and DOE EEMS projects. The focus of these projects is to validate the energy-saving potential of various CAV technologies. To meet the research objectives of the projects these vehicles were instrumented with various sensors and a data acquisition system. The vehicle instrumentation architecture is shown in Figure 5. The vehicle instrumentation consists of a dSPACE MicroAutoBox II (MAB II), serving as an on-board processing unit for vehicular controls and a high-resolution data acquisition system. It also interfaces with various CAN channels of the vehicle and auxiliary sensors in the instrumentation package. SWIFT GPS unit, New Eagle drive-by-wire system, and various analog sensors are attached to the MAB II. A detailed summary of the vehicle instrumentation is laid out in Table 3.



Figure 5 Vehicle Instrumentation in boot

Table 3 Vehicle Instrumentation details

S.No.	Component	Description
1	MABx	dSPACE Controller – Controller integration and data acquisition system
2	DBW module	Drive-by-Wire system controller
3	Leddar VU8	Obstacle detection
4	Delphi Radar	Obstacle detection
5	Cohda Radio	Processing BSM, MAP, and SPaT information
6	GNSS module	Obtaining vehicle's current location
7	GNSS Antenna	Obtaining accurate position information
8	IMU	Obtaining vehicle orientation

A laptop is also connected to the MAB II as shown in Figure 6, to provide a human-machine interface for real-time control and actuation of the vehicle instrumentation.

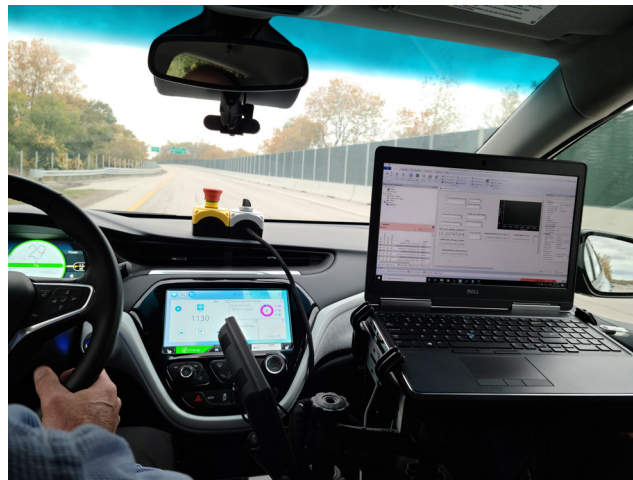


Figure 6 Laptop connected to vehicle performing real-time vehicular control.

3.2 Data collection

3.2.1 On-road data collection

3.2.1.1 MTU drive cycle

Michigan Technological University Drive Cycle (MTUDC) is an amalgamation of city and highway driving. The drive cycle stretches up to 24 miles and nearly experiences 160 m of elevation change happening multiple times. The drive cycle is designed such that it has five different signalized intersections, and the drive cycle has the capability to stop the vehicle six times on these five intersections. The drive cycle is an anticlockwise closed-circuit starting and ending at APS Labs. The circuit has twelve right-hand turns and eight left-hand turns. The drive cycle laid over the map is shown in Figure 7. Further details of the drive cycle can be found in [17].

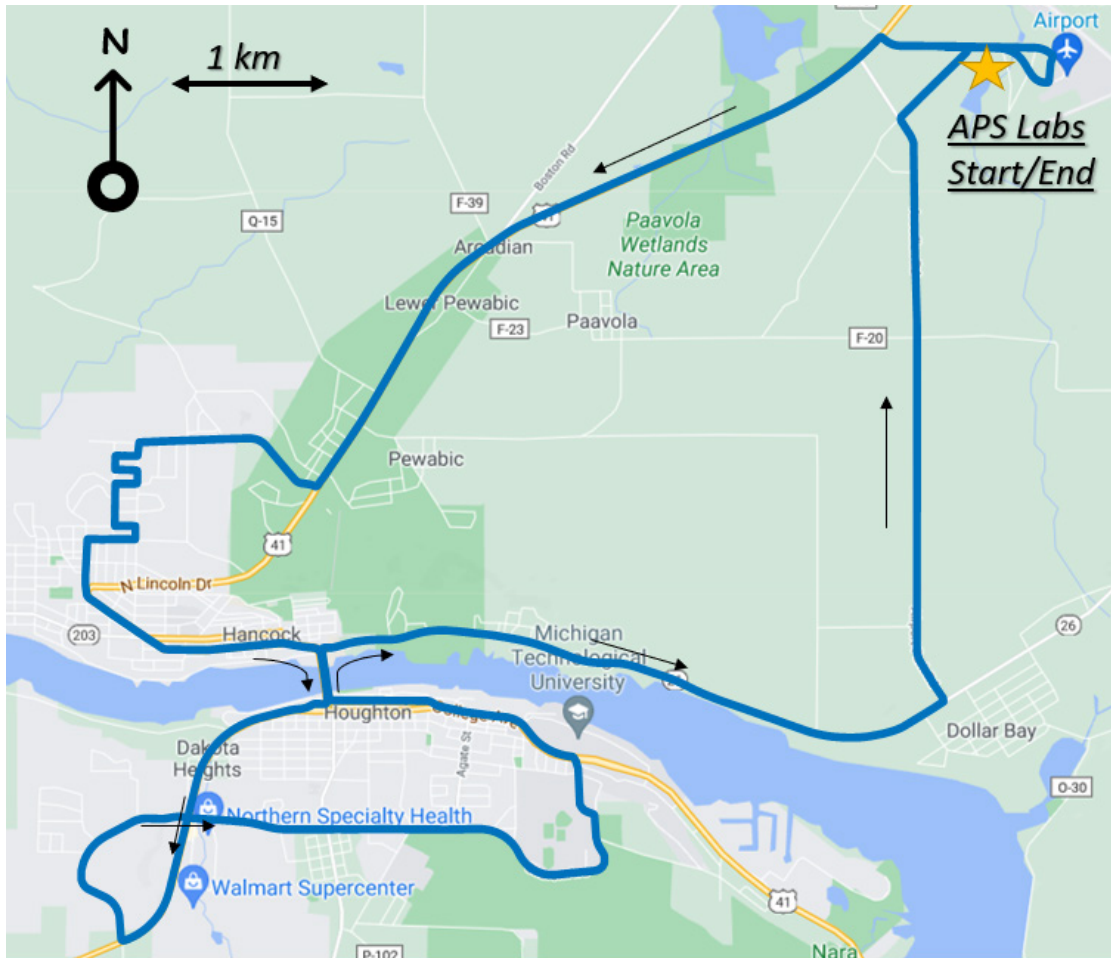


Figure 7 MTU Drive cycle, original image taken from Google maps.

The MTU drive cycle comparison to standard EPA drive cycles is shown in Table 4. The MTU drive cycle features an average speed of 33 MPH which lies in between the UDDS and other high-speed drive cycles. However, the MTU drive cycle is the longest of all the other drive cycles with a total distance of 24 MPH.

Table 4 MTU drive cycle comparison with EPA standard drive cycles

Drive Cycle	Distance (mi)	Average speed (mph)	Maximum speed (mph)
UDDS	7.5	20.1	56.7
HWFET	10.3	49.1	60.0
US06	8.0	49.7	80.3
MTUDC	24.0	33.0	55.0

3.2.1.2 *RSU loop*

To demonstrate the energy-saving potential of Eco-AnD, a subset corridor of the MTUDC was chosen with all the intersections. The distance of this corridor is 7 miles and has an elevation change of 136.6 m. The maximum speed around this corridor is 45 mph and the minimum speed is 25 mph. The description of each intersection is given in Table 5.

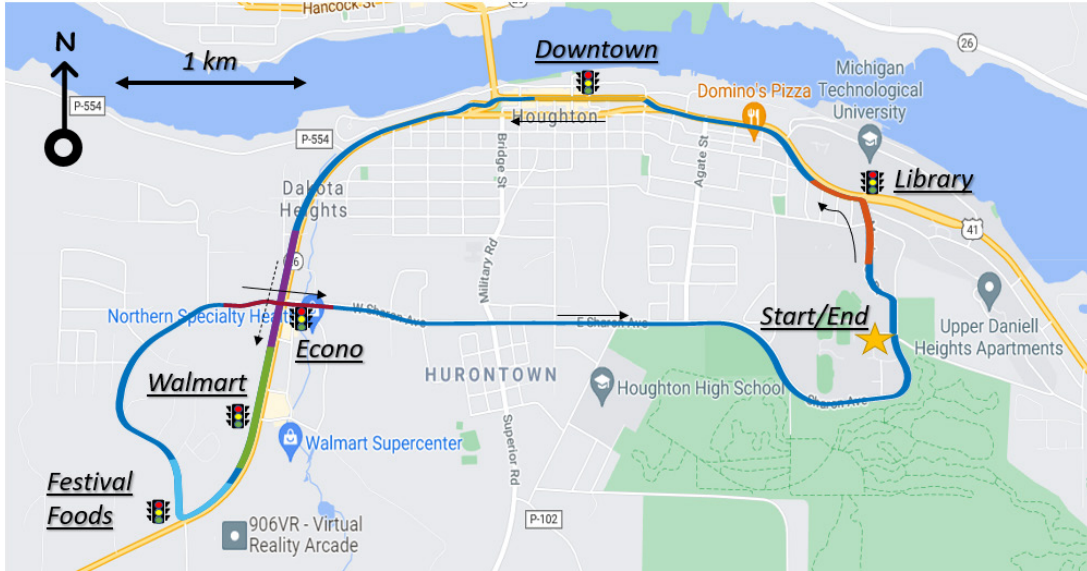


Figure 8 RSU loop, original image taken from Google maps.

The corridor in Figure 8 shows the RSU loop. The five intersections can be seen and the approach and departure distances for each intersection are shown with the color. For example, the library intersection is shown in orange. The distance before the traffic light is the approach and the distance after the traffic light is the departure distance. It can also be observed that the Econo intersection is crossed twice first from going from downtown to Walmart (direction - southbound) and the second time while going from festival foods to the library (direction - eastbound).

Table 5 RSU loop intersection details

Intersection	Approach Distance (m)	Departure Distance (m)	Speed limit - Approach (mph)	Speed limit - Departure (mph)	Phase Timings (s)		
					Green (5)	Red (3)	Yellow (7)
Library	300	300	25	30	25	40	4
Downtown	300	300	25	25	32	28	4
Econo South Bound	300	300	45	45	21	43	4
Walmart	300	300	45	45	32	32	4
Festival Foods	300	300	45	25	22	44	4
Econo East Bound	300	300	25	35	21	43	4

The phase timings of the signals in Table 5 are the observed values at the intersection. These values are then used to simulate the results for the Eco-AnD algorithm. The road elevation change in these intersections is detailed in Table 6.

Table 6 RSU loop intersection elevation details

S.No	Intersection	Elevation at -300m	Elevation at 300 m	Elevation change
1	Library	207.6	177.3	-30.3
2	Downtown	165.9	160.0	5.9
3	Econo South Bound	198.4	224.4	26.0
4	Walmart	222.9	248.8	25.9
5	Festival Foods	252.4	278.3	25.9
6	Econo East Bound	227.9	216.6	-11.3

From the elevation change with respect to distance, the road grade can be easily calculated. The grade across these intersections varies from -6.8 deg to +4.1 deg. The plot for the grade of each intersection is shown in Figure 9. These grade values are used as the disturbance signal to the Eco-AnD algorithm to consider the road dynamics.

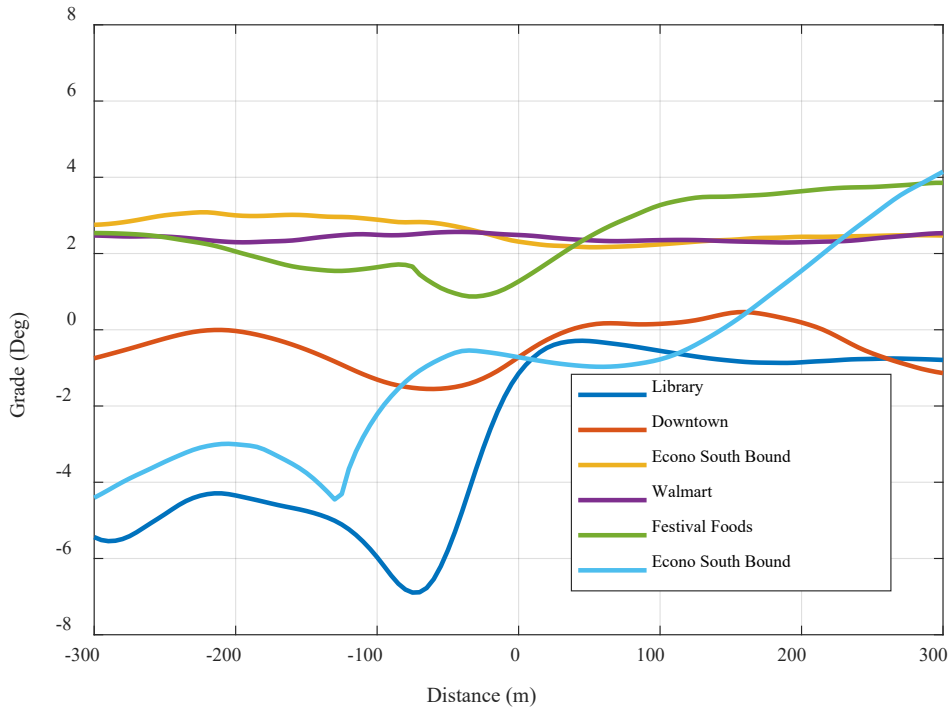


Figure 9 RSU loop Intersection Grade

3.2.2 Track data collection

Track data for Chevrolet Volt Gen II was collected at the American Center of Mobility (ACM). The track consists of 2 intersections with DSRC communication to broadcast SPaT and MAP information. Optimized speed profiles were tested at these intersections to validate the energy savings by the developed Eco-AnD algorithm.

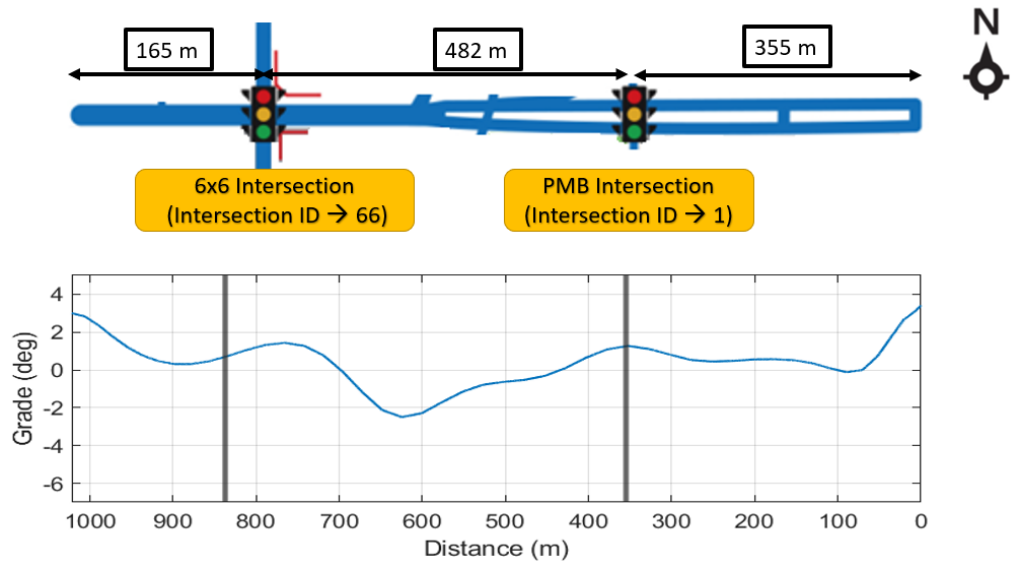


Figure 10 ACM Intersection Map

The phase timings for the intersections at ACM are observed values and summarized in Table 7.

Table 7 ACM Intersection details

S.No	Intersection	Approach Distance (m)	Departure Distance (m)	Speed limit - Approach (mph)	Speed limit - Departure (mph)	Phase Timings (s)		
						Green	Red	Yellow
1	6x6	300	165	35	35	25	47	4
2	PMB	300	300	35	35	25	19	4

4 Model Development

The Eco-AnD model is developed in MATLAB. Open-source MATLAB function “DPM” is used to develop the dynamic programming-based algorithm [18]. The function takes the inputs of the cost function, constraints, states, control inputs, and disturbances, if any, and runs the Bellman-Ford algorithm for backward dynamic programming. The problem has been designed in the domain of distance from the intersection, as described in Figure 11, where distance before the intersection (approach distance) is negative, zero at the intersection, and positive after crossing the intersection (departure distance). DSRC communication range of 300 m before the intersection is assumed while defining the problem.

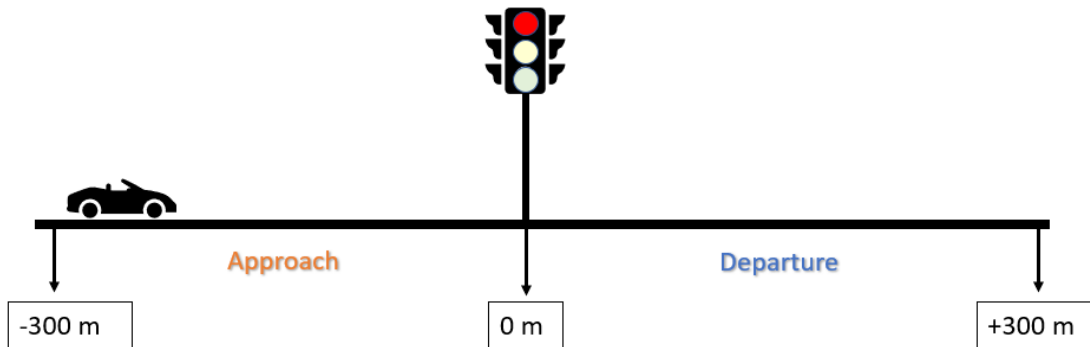


Figure 11 Distance from intersection description

4.1 Dynamic programming and its components

As described previously, the inputs to the DP are the cost function, constraints, states, control inputs, and disturbance signals. The problem length is dependent upon the

approach and departure distance. A discrete level of 5 m is chosen for performing the DP calculations considering the computation time.

4.1.1 Inputs to DP

Figure 12 gives a pictorial description of the inputs to the DP. It can be observed that as soon as the vehicle enters the DSRC range of intersection, it begins to receive the SPaT and MAP messages broadcasted by the roadside unit (RSU). Having access to the vehicle's CAN information vehicle has all the information required to process the inputs to the DP. Table 8 gives detailed information on the inputs to the DP.

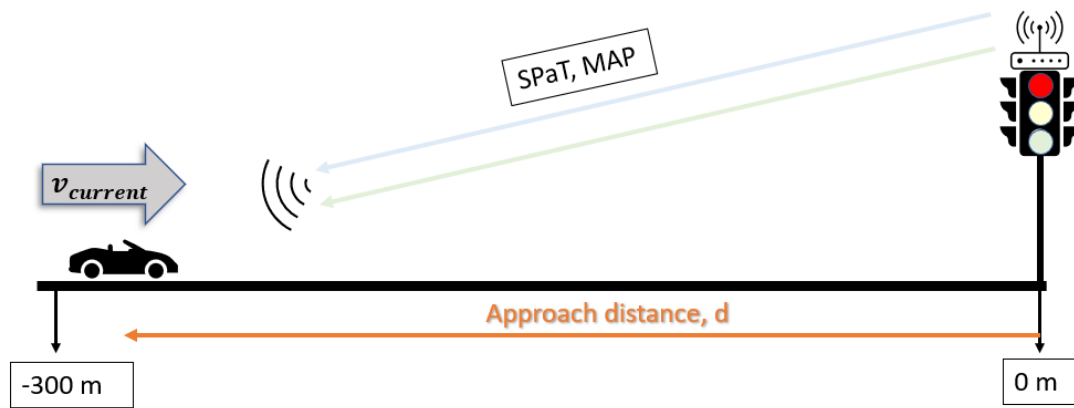


Figure 12 Pictorial view of inputs to DP

Table 8 Summary of inputs to DP

S.NO	DP Parameter	Physical Entity	Source of information
1	States	State 1: Velocity (m/s) State 2: Time (s)	State 1: Vehicle CAN State 2: Calculated

2	Control Input	Acceleration (m/s ²)	Derived from velocity
3	Domain	Distance (m)	Combination of MAP data and vehicle's GPS
4	Constraints	Constraint 1: Cross intersection in green phase Constraint 2: Maintain the legal speed limit	Constraint 1: SPaT information (current phase, time to next color) Constraint 2: MAP information
5	Disturbance	Road grade (Deg)	

Inputs to the DP are given in the form of a grid to perform the Bellman-Ford optimization. The grid discretization is summarized in Table 9.

Table 9 Discretization of inputs to DP

S.No	Input	Minimum limit	Maximum limit	Discrete level
1	State 1: Velocity	0 m/s	Max legal speed limit in m/s	0.2 m/s
2	State 2: Time	0 s	Max time for green phase closing + 20s	0.1 s
3	Control input : Acceleration	-3.0 m/s ²	+3.0 m/s ²	0.1 m/s ²

4.1.2 Cost function

The cost function to the DP is the way of describing the system in DP. The DP aims to minimize energy consumption, so the cost function must be defined such that the EGO vehicle's energy consumption is related to the states and control input. As described in 2.3, the cost function to the DP is the reduced-order energy model. For Chevrolet Volt Gen II, the CD model energy model is used for developing the Eco-AnD algorithm. The equation for the model can be found in (1) & (2). For GM Bolt the reduced-order model development is explained in section 4.3. The flow of calculating the cost function is shown in Figure 13.

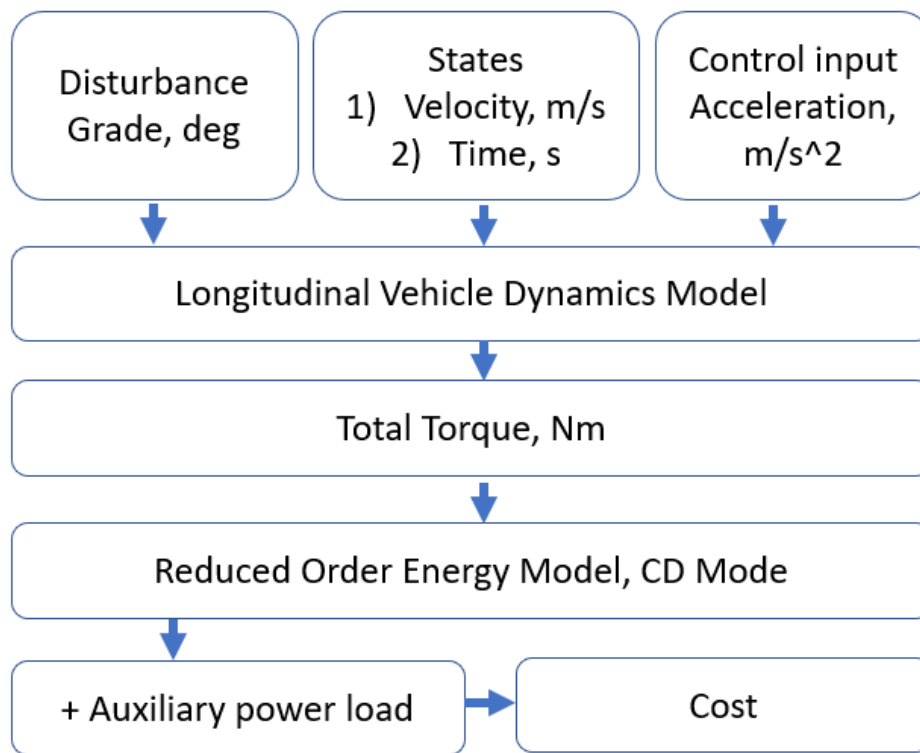


Figure 13 Schematic for calculation cost function - Volt

The cost estimation process can be generalized for any vehicle powertrain architecture given that the reduced-order energy model is available to use. For the current study, the reduced-order energy model for both the vehicle takes the input of road grade and vehicle velocity. Using these inputs, the cost for each iteration can be calculated. Vehicle auxiliary power may also vary from vehicle to vehicle. For this study, a constant auxiliary power load of 1.5 kW is assumed.

To describe the vehicle's model and calculate the cost for a discrete level following calculations are made-

Step 1: Calculate final speed from control input and initial speed for 5 m.

$$v = \sqrt{u^2 + 2a * 5} \quad (3)$$

Step 2: Calculate the time taken for the maneuver and the total time.

$$t_k = \frac{5}{u} \quad (4)$$

$$T_k = t_k + T_{k-1} \quad (5)$$

Step 3: Calculate axle torque for the maneuver.

$$\alpha = \frac{a}{r} \quad (6)$$

$$F_{inner} = \frac{I_{eff} * \alpha}{r} \quad (7)$$

$$T = (F_0 + F_1v + F_2v^2 + Ma + F_{inner} + Mgsin(\theta))r \quad (8)$$

Step 4: Calculate the cost.

$$E = C_1 + C_2T + C_3v + C_4Tv + C_5T^2 + C_6v^2 \quad (9)$$

$$C = E.dt + 1.5.dt \quad (10)$$

4.1.3 Constraints to DP

Constraints to DP are mathematical inequality equations used to describe any physical constraint that is the vehicle is required to follow. For the case of Eco-AnD, these constraints are described in Table 10.

Table 10 Constraints to DP

S.No.	Physical Constraint	Mathematical form
1	Road speed limit	$v < v_{limit}$
2	Cross intersection in green phase	$t_{cross} > t_{open}$ & $t_{cross} < t_{close}$ Where t_{cross} is the time to cross the intersection and t_{open} is the time for the next green phase to start and t_{close} is the time for the next green phase to finish.

To calculate the variables t_{open} and t_{close} information for the SPaT message is used. The signal “minEndTime” gives the time for the next color change and the signal “currentphase” is descriptive of the current phase of the traffic signal, as described in appendix 7.1. Combining this information at a -300 m distance from the intersection, a feasible green phase passing window can be calculated. A detailed explanation of

possible cases is explained in Table 11. Abbreviation t_{rem} is used to depict the time to the next color change.

Table 11 Passing window timing calculations.

S.No	Situation	Equations for passing window opening	Equation for passing window closing
1	Current phase = Red (3)	$t_{open} = t_{rem}$	$t_{close} = t_{rem} + t_g$
2	Current phase = Green (5)	$t_{open} = 0$	$t_{close} = t_{rem}$
3	Current phase = Yellow (7)	$t_{open} = t_{rem} + t_r$	$t_{close} = t_{rem} + t_r + t_g$

The pictorial representation of the passing window calculation is shown in Figure 14. Open and closing window of the passing phase is shown in each case of the current phase. For example, the case in the image shows the passing window when the current phase is red (3). The passing window opens when the signal changes from red to green and closes when the green phase changes to yellow. For each case, an illustrative example is shown demonstrating one of many possible vehicle trajectories to cross the intersection in the green phase passing window.

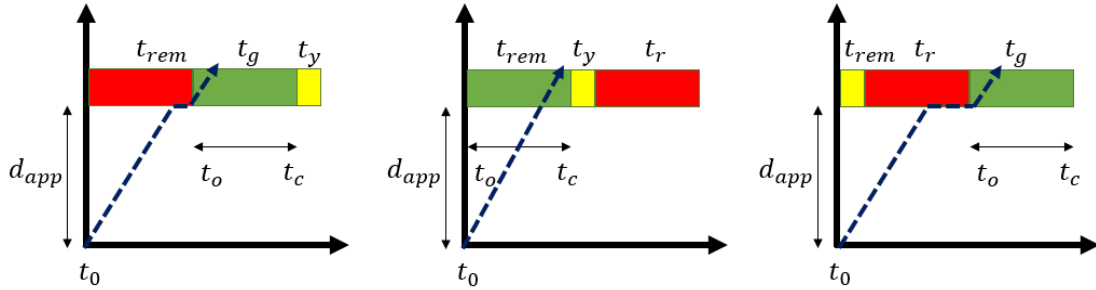


Figure 14 Pictorial representation of passing window calculation

4.1.4 Simulation Results for GM-Volt Gen II

To observe the working of the algorithm, the 6x6 intersection at ACM proving grounds was designed in simulations. Using the grade information from Figure 10 and phase timings from Table 7 inputs of disturbance signal and SPaT signal were simulated. The current phase and time to next color signals were chosen from one of the manual-driven test runs, detailed in Table 12.

Table 12 6x6 intersection physical scenario

Intersection	6x6
Current Phase	Red
Time to next color	32 s
Grade change	-2.1 to 2.4 deg
Speed limit	35 MPH
Approach distance (m)	300
Departure distance (m)	165

Using these values, the results from the Eco-AnD algorithm can be obtained as shown in Figure 15.

Subplot 1 shows the optimized speed vs distance plot. As it is established in Table 7, the departure distance of the intersection is 165 m which gives a total distance of 465 m for the intersection. At the entrance of the intersection, distance = -300, the speed of the vehicle is 35 MPH and drops to 17 MPH before reaching the intersection. This speed drop can be explained by observing subplot 2 that shows the relation of travel time vs distance. To avoid crossing the intersection during the red phase, the vehicle slows down and only crosses the intersection once the signal switches to the green phase which happens at 32 seconds. Subplot 3 shows the trend of control input (acceleration) to the dynamic programming algorithm, and throughout the intersection, the acceleration stays within -1.1 m/s^2 and 0.6 m/s^2 . The subplot shows the energy expenditure by the vehicle which also is the minimum cost for the maneuver as generated by the dynamic programming algorithm. Total energy expenditure at the end of the maneuver is 258.3 kJ.

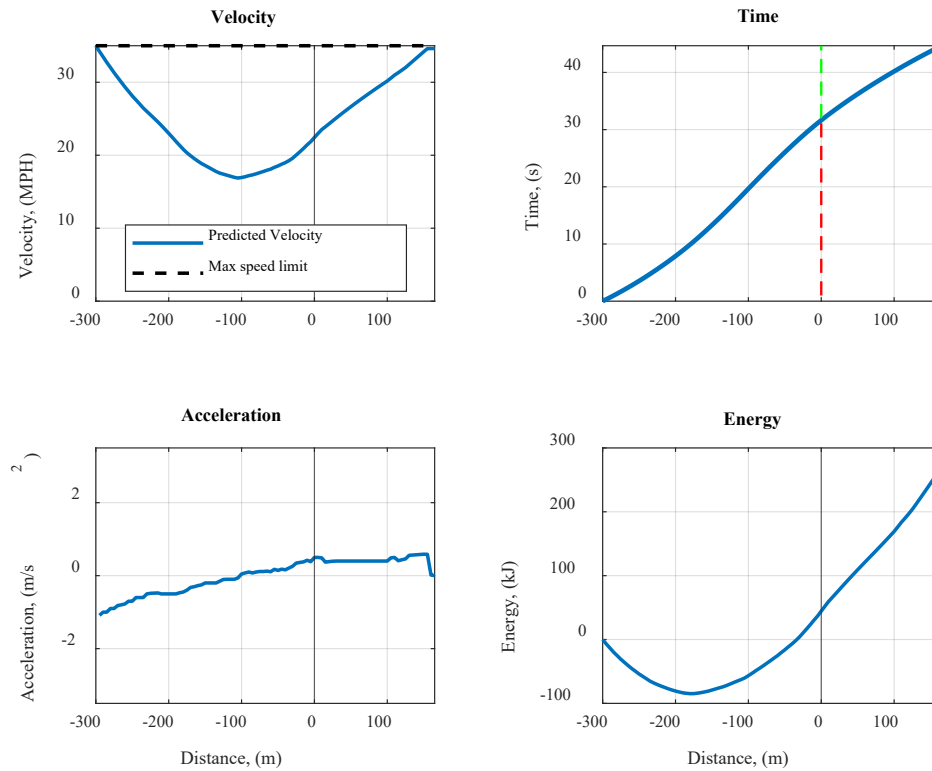


Figure 15 Simulation result for 6x6 intersection

4.2 Baseline model development

One of the distinguished benefits of CAV technologies is their energy-saving potential. From the literature review in section 2.2, it can be concretely said that the Eco-AnD algorithm can save considerable energy for crossing the intersection depending upon the factors such as type of speed profile optimizer, road conditions, and vehicle powertrain. So, estimating the energy-saving potential of the developed algorithm proves to be one of the key elements of the research progression. To estimate the energy consumption improvement, the comparison of energy consumption of

optimized speed profiles must be made against the human-driven maneuvers. This research focuses on estimating the energy savings in simulations as well as in real-life testing. Details on real-life energy savings by the Eco-AnD algorithm are explained in section 5.

Human driving patterns vary from person to person. In [19, 20] authors have developed several models to mimic human driving patterns in simulations. Their basis of study includes studying the acceleration and deceleration patterns of human driving for both straight roads and curved roads. Out of several models developed by them, constant acceleration and deceleration models are chosen for studying the energy benefits of the Eco-AnD algorithm. Running several experimental tests, they have found out the acceleration and deceleration patterns can be approximated to constant numbers. The average acceleration value can be approximated to be equal to 1.25 m/s^2 and the average deceleration can be approximated to be -1.4 m/s^2 . Also, their experimentation with different reference speeds shows that the speed limits do not have a significant influence on the driver's acceleration patterns.

To further examine the acceleration and deceleration values analyses were made on EPA standard drive cycles [21]. Out of various EPA drive cycles, three drive cycles were chosen that would cover most of the human driving patterns. EPA Urban dynamometer drive cycle (UDDS) was used to analyze the city driving patterns. The drive cycle features various stop-and-go maneuvers to replicate heavy traffic driving followed by some high-speed maneuvers reaching up to 60 MPH. Second, the Highway fuel economy drive cycle (HWFET) was used to analyze the highway speeds

driving patterns. Third, the US06 drive cycle was used to analyze the aggressive driver behavior. This drive cycle features various aggressive speed increase/decrease and stop and go maneuvers to mimic an aggressive driving behavior. The acceleration vs speed relation for these three drive cycles can be observed in Figure 16.

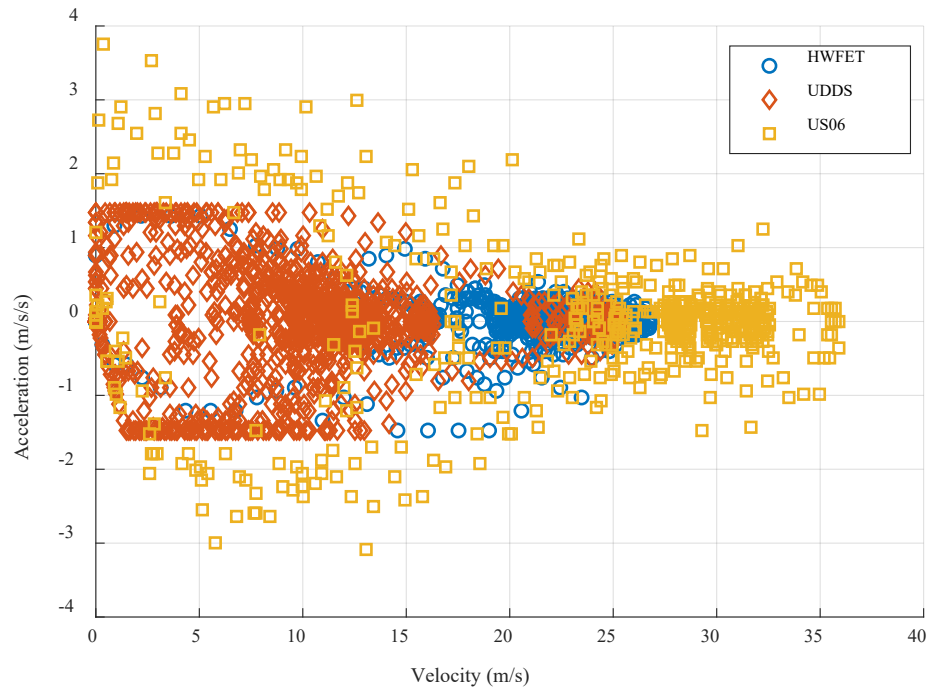


Figure 16 EPA drive cycles speed vs acceleration scatter plot

From Figure 16, the overlook of the plot of the trends on acceleration for different driving conditions can be seen. Using this data, the acceleration and deacceleration values can be found for an average driver as well as for an aggressive driver for speeds less than 45 MPH. The summary of these values can be found in Table 13.

Table 13 EPA drive cycles avg acceleration and deacceleration

S.No.	Drive Cycle	Driver Behavior	Avg Acceleration	Avg

				Deacceleration
1	UDDS	Normal driver - City	1.04 m/s ²	-1.45 m/s ²
2	HWFET	Normal Driver - HW	0.98 m/s ²	-0.45 m/s ²
3	US06	Aggressive Driver - City	2.33 m/s ²	-2.05 m/s ²

Using these acceleration and deacceleration values an estimate of human driving can be made by assuming the human speed change maneuver to be a constant acceleration maneuver. An example of such a case is shown for the same real-life case as explained in Table 12. The speed profile is developed keeping in mind that the driver has no knowledge of the intersection phase timings beforehand. The driver is aware of only the current phase state of the intersection (color of traffic light) as perceivable. As a normal driver behaves at a traffic light, the simulated speed profile first maintains the constant speed till the vehicle is close enough to the traffic light to manually apply the brakes and bring the vehicle to a complete stop. After that, the speed profile is held a zero speed till the current phase of the traffic light changes from red to green and the vehicle begins to accelerate back to the speed limit of the road. Once the speed limit is reached then the vehicle maintains the speed limit and crosses the departure distance of the intersection. For both the acceleration and deacceleration for this maneuver constant values are assumed from the EPA drive cycle analysis for urban city driving.

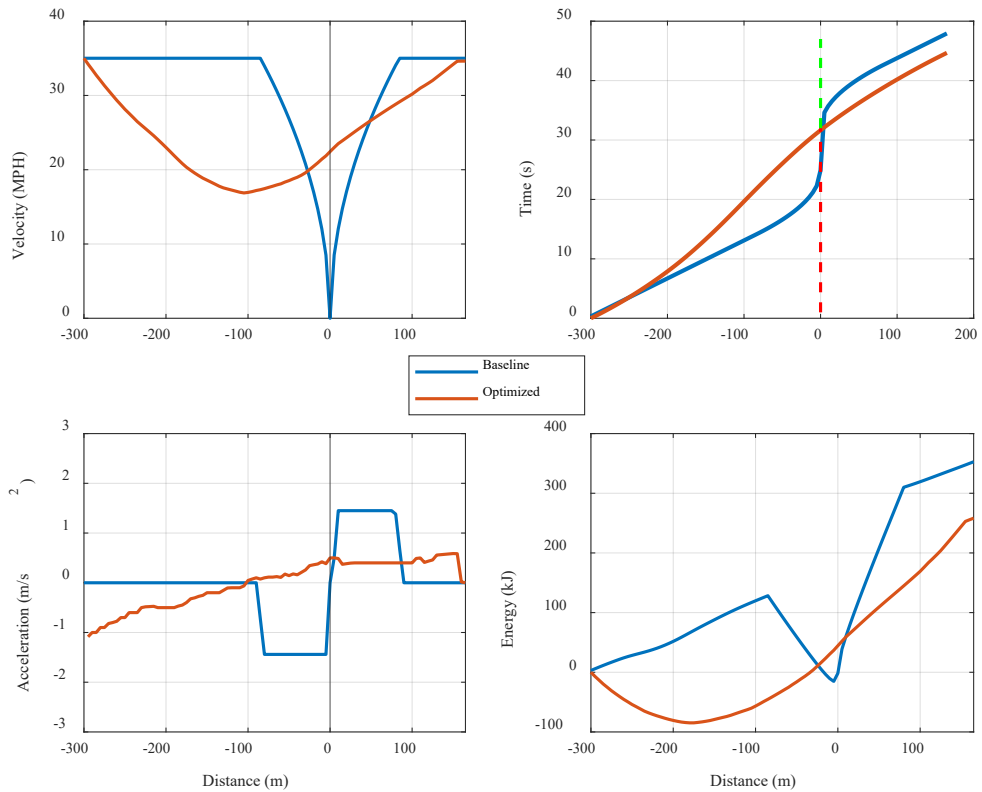


Figure 17 6x6 intersection baseline comparison - Volt

In Figure 17, the comparison of the simulated baseline speed profile is made with the Eco-AnD algorithm optimized speed profile. The baseline speed profile in subplot 1 is developed by using a constant acceleration and deceleration value for vehicle speed change maneuver for human driving.

Subplot 2 shows that the time to cross the intersection for both the speed profiles is almost the same, 32.2 seconds, right after the traffic phase changes to green. From Subplot 3, the acceleration pattern of both the maneuvers can be seen and it is to be noted that the constant acceleration and deceleration are assumed while designing the

baseline speed profiles. It can also be observed that the Eco-AnD algorithm generated speed profile takes lesser time to cross the intersection as compared to the baseline case. From subplot 4, the comparison of energy consumption can be observed. The energy estimates are done using Volt's reduced-order model that is used as the cost function for the DP algorithm, described in (10). The energy benefit for this scenario is 73.1 kJ or 20.7 %. By doing a similar analysis the energy-saving potential for other intersections can be estimated as well.

The calculations made for developing the speed profile are as follows:

Step 1: Calculating the stopping distance for given deacceleration of -1.45 m/s^2 from an initial speed of 35 mph (15.65 mps)

$$d_{stop} = \frac{(v^2 - u^2)}{2a} \quad (11)$$

$$d_{stop} = \frac{0^2 - 15.65^2}{2 * (-1.45)} = 84.5 \text{ m} \quad (12)$$

Step 2: Calculate the constant speed region for approaching the intersection.

$$d_{cs,app} = 300 - d_{stop} = 300 - 84.5 = 215.5\text{m} \quad (13)$$

Step 3: Calculate distance for accelerating back to 35 mph (15.65 m)

$$d_{accel} = \frac{(v^2 - u^2)}{2a} \quad (14)$$

$$d_{accel} = \frac{15.65^2 - 0^2}{2 * (1.45)} = 84.5 \text{ m} \quad (15)$$

Step 4: Calculate distance for constant speed during departure.

$$d_{cs,dep} = 165 - d_{accel} = 165 - 84.5 = 80.5\text{m} \quad (16)$$

Step 5: Once all the distances are found then using the reduced energy model for GM-Volt Gen II, the energy consumption is calculated for the maneuver.

4.3 Bolt- Eco-AnD Algorithm Development

Energy estimation plays a key role in developing the CAV technologies, as is the case for the Eco-AnD algorithm. For GM-Volt Gen II, the reduced-order energy estimation model was used as the cost function for the dynamic programming algorithm so for developing the similar Eco-AnD algorithm for GM Bolt, a reduced-order model is developed. The reduced-order model was developed using the dynamometer testing data provided by Argonne National Laboratory (ANL) to MTU as a development resource for the DOE EEMS project.

4.3.1 Reduced-order energy model development process

A reduced-order energy model for a fully electric vehicle (Bolt) should be analogous to the energy model used in (9) for the CD mode of GM Volt Gen II. A reduced-order model can be visualized as a two-dimensional response surface where the predictor variables are vehicle velocity and axle torque, and the response variable is high voltage battery power consumption. The general equation for a second-order response surface for this application is shown in (17).

$$Power_i = P(1) * T^2 + P(2)T * V + P(3) * T + P(4) * V^2 + P(5) * V + P(6) \quad (17)$$

The reduced-order energy model development process can be characterized into four broad steps.

4.3.1.1 Step 1: Understanding the data

The dynamometer data used for developing the reduced-order energy model for Bolt comprises eight drive cycles. These drive cycles consist of various EPA standard drive cycles such as UDDS, US-06, HWFET, and NEDC (Figure 18).

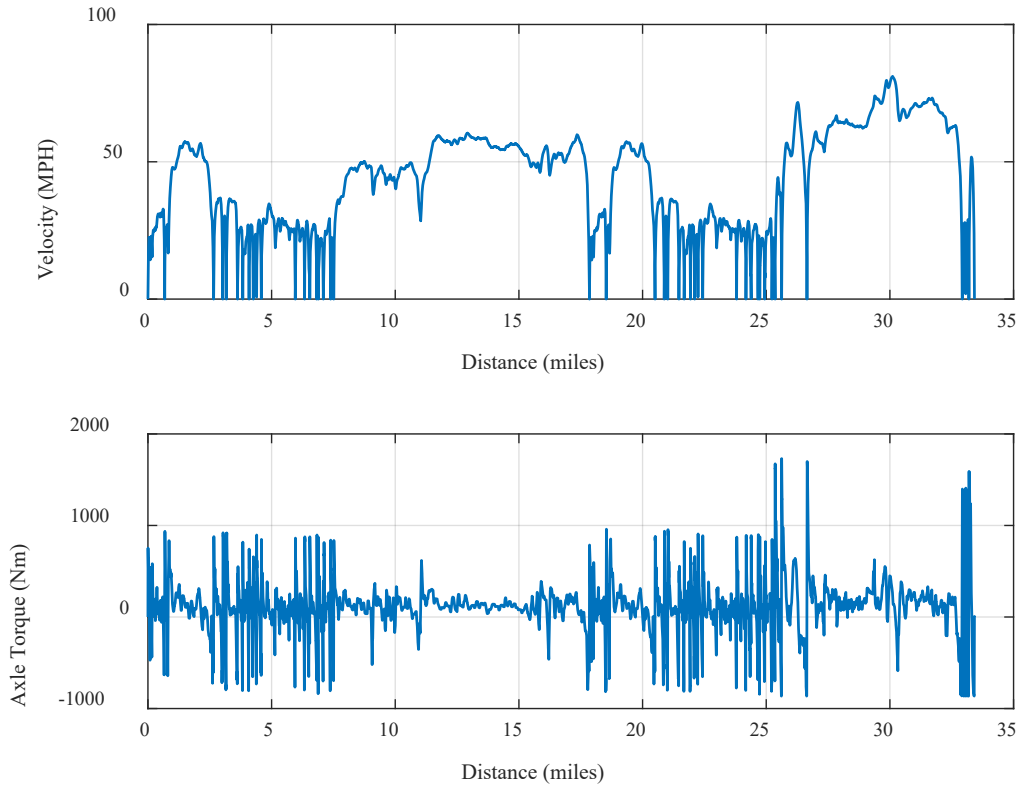


Figure 18 Dynamometer drive cycle with EPA drive cycles

EPA drive cycles alone capture most of the on-road driving behaviors for an average driver. The dynamometer drive cycles also contain drive cycles that capture various aggressive acceleration and braking maneuvers to collect the data on high power

regions of the high voltage battery. One such example of a drive cycle is shown in Figure 19.

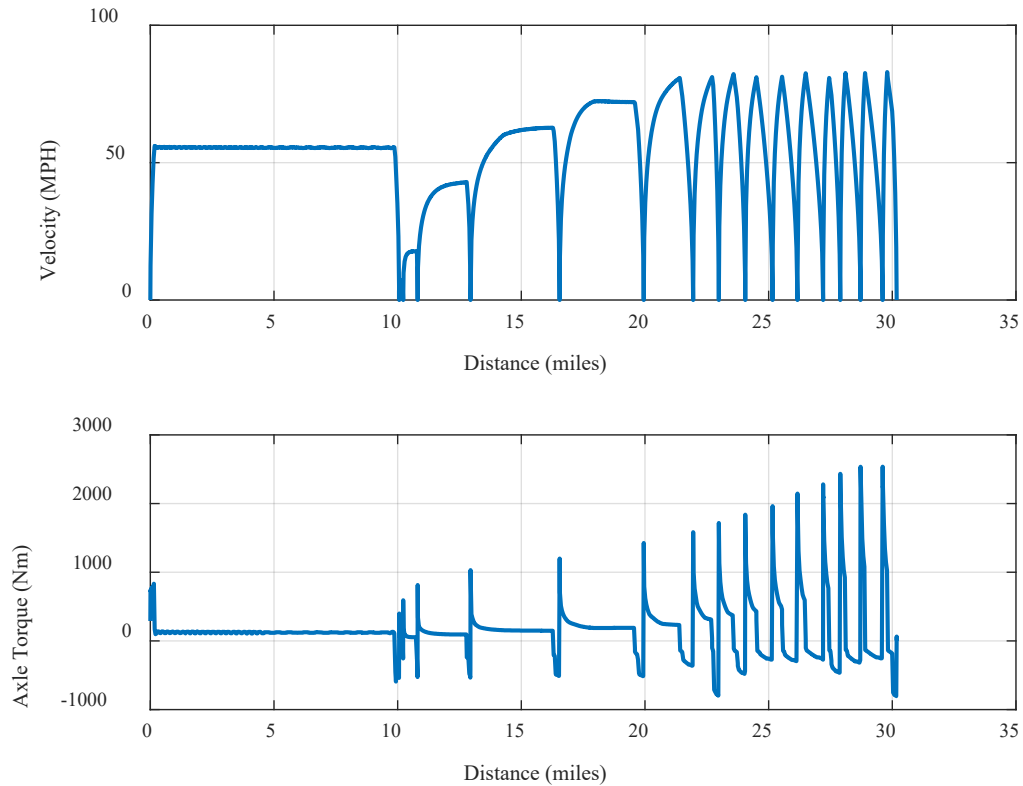


Figure 19 Dynamometer drive cycle with aggressive acceleration and braking

4.3.1.2 Step 2: Understanding the powertrain efficiencies.

Before developing the response surface from the dynamometer data, understanding the vehicle's powertrain is one of the crucial elements. The Bolt has a permanent magnet synchronous motor powering the front wheels with a fixed final drive ratio. A motor of this sort typically has varied efficiency regions based upon the torque it is delivering

the speed it is running at, called operating points. The efficiency map of a PMSM motor of Bolt can be found in [22].

At low torque regions, the efficiency of the motor decreases as torque approaches zero. The efficiency of the PMSM machine also varies depending upon if the machine is being used as a motor or generator. To account for these factors the efficiency map of the motor is divided into different segments, described in Table 14, to develop the response surfaces for the reduced-order energy model.

Table 14 Bolt Motor torque regions

Torque Zone	PMSM Torque Zone	Axle Torque Zone	Motor Operation
1	$T_m < 0$	$T_{axle} < 0$	Generator
2	$0 < T_m < 63.8$	$0 < T_{axle} < 450$	Motor
3	$T_m > 63.8$	$T_{axle} > 450$	Motor

4.3.1.3 Step 3: Developing the response surface from the dynamometer data.

To develop the response surface, first, the data for vehicle speed, axle torque, and battery power was collected from all the drive cycles. Based upon the torque zones described in step 2, the data for bifurcated into three different groups. Using MATLAB, a second-order surface was developed to fit the data in an individual group that has the velocity on the x-axis, axle torque on the y-axis, and battery power on the z-axis. The fitted response surface generates the coefficients for each variable in equation (17). The results for the coefficients are shown in Table 15.

Table 15 Bolt Power coefficients for energy model

Power coefficient	Torque Zone 1	Torque Zone 2	Torque Zone 3
P1 ($\frac{W}{Nm^2}$)	0.0021	0.0111	0.0037
P2 ($\frac{W}{Nm*s/s}$)	3.1966	3.4336	3.7041
P3 ($\frac{W}{Nm}$)	0.1140	-2.9763	-6.7324
P4 ($\frac{W}{(m/s)^2}$)	2.2523	-2.5400	9.7436
P5 ($\frac{W}{m/s}$)	3.2761	92.3184	-424.2011
P6 (W)	527.8151	265.2647	4887.3000

4.3.1.4 Step 4: Validating the developed response surfaces.

Once the response surfaces were developed, the developed reduced-order model was used to predict the energy consumption for the dynamometer drive cycles. To predict the energy equation (18) is used. The result for the dynamometer drive cycles with EPA drive cycles is shown in Figure 20.

$$E = \sum_{k=1}^n P_{pred,k} * dt \quad (18)$$

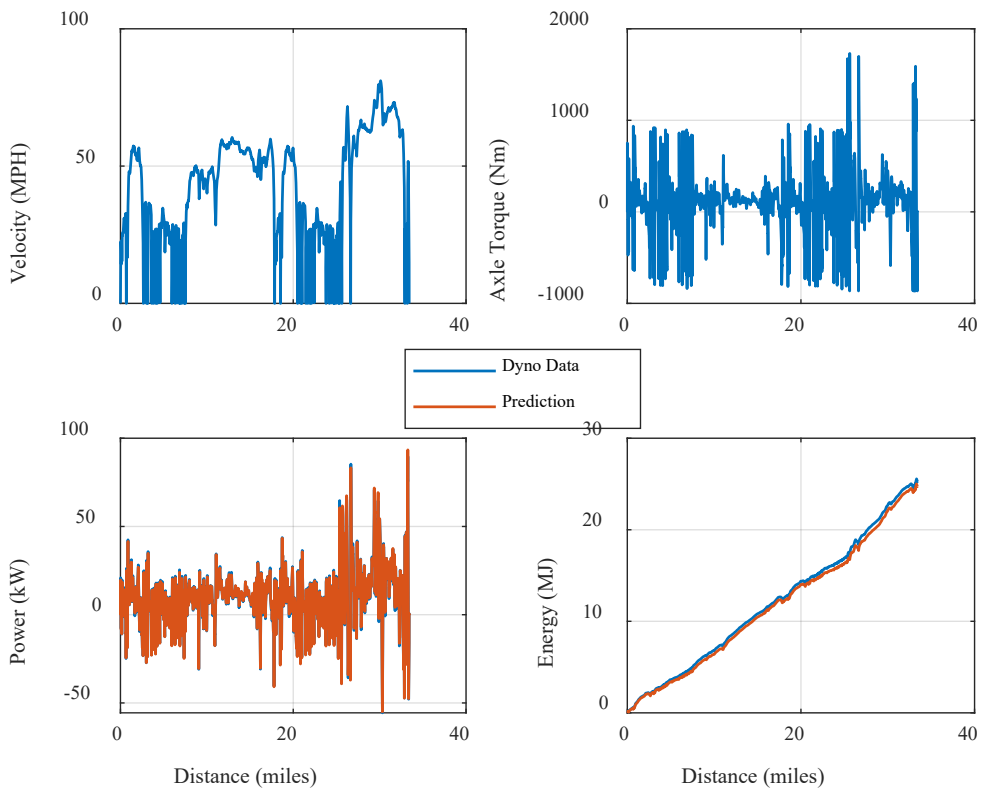


Figure 20 Bolt reduced-order energy model result.

For the eight drive cycles, the model has an accuracy of over 93% and the detailed results for all the drive cycles are shown in Table 16.

Table 16 Bolt- Dynamometer energy prediction results

DC	Distance (miles)	Max Energy Predicted (MJ)	Max Energy Data (MJ)	Error %	MPGe Predicted	MPGe Data
1	28.9	23.4	23.2	0.7	153.2	154.4

2	13.8	9.9	10.1	-1.6	179.6	176.8
3	13.2	13.2	13.3	-1.0	127.6	126.4
4	30.2	27.5	27.9	-1.4	136.9	134.9
5	7.8	6.9	7.0	-1.0	137.9	136.6
6	33.4	25.7	25.6	0.4	159.8	160.5
7	180.8	177.9	166.8	6.8	123.5	131.8
8	22.3	20.7	19.6	3.9	136.8	122.1

4.3.2 Brake Blending strategy

For a conventional vehicle, the kinetic energy loss during the braking event is typically lost in the form of heat generated by the friction brakes. But with the electrification of the vehicles, harnessing this kinetic energy has been possible. Most of the PHEVs and electric vehicles can convert the kinetic energy to chemical energy in the battery. The traction motor that is used for propelling the vehicle can also be used as a generator to harness the energy.

Electric vehicles are equipped with both regenerative braking as well as mechanical friction braking. Since regenerative braking may not be sufficient during all the braking scenarios certain blending strategies are incorporated to provide a blend of friction brakes and regenerative braking. Factors such as inefficiency of motor/generator at certain operation points, brake torque demand more than peak torque output of motor/generator unit and reduced life of powertrain components play a crucial role in decoding the blending strategy for a vehicle.

For GM Bolt the brake blending strategy was figured out by analyzing the dynamometer testing data. EPA drive cycle (UDDS, HWFET, US06) was used for analyses as they capture most of the human driver braking patterns, Figure 21. Dynamometer data is used for analysis as it has lower noise factors of road grade and wind.

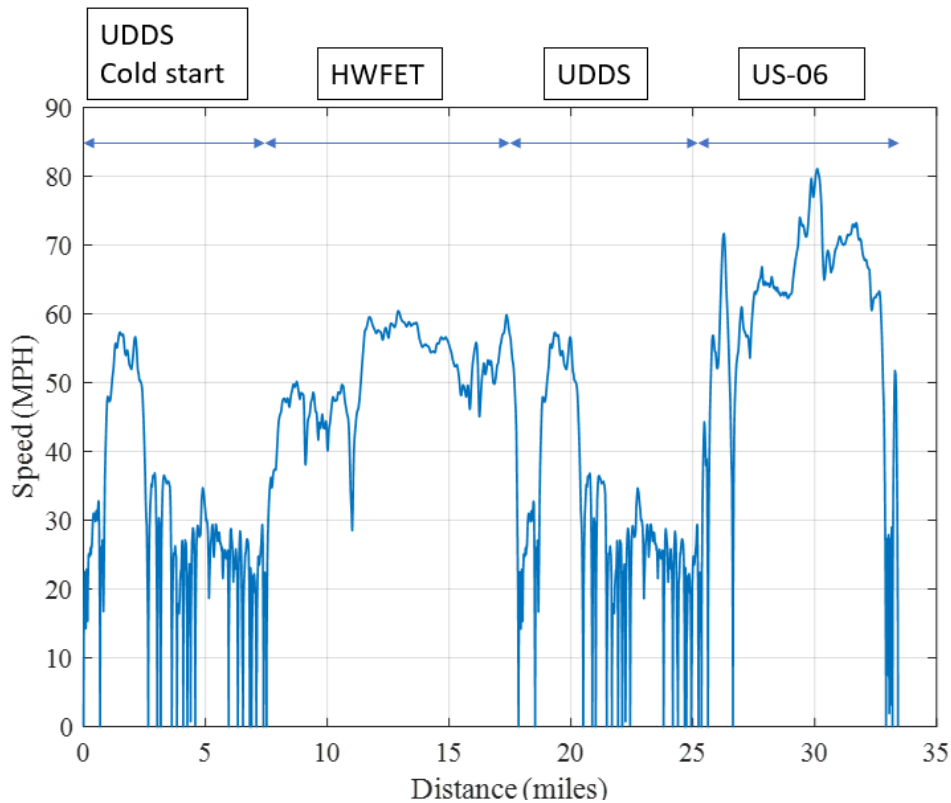


Figure 21 Drive cycle for brake blending analysis.

For performing brake blending analysis vehicle's CAN data is used. Information of vehicle speed and regenerative torque is obtained from the vehicle's primary CAN and used for the analysis. Total braking torque of the vehicle is estimated using longitudinal vehicle dynamic model for the vehicle, as stated in (19), where F_0, F_1, F_2

are the set coefficients for the GM Bolt 2019 [23]. Brake blending factor (BF) is defined as the proportion of the braking effect due to regenerative braking in comparison to total braking torque. The mathematical expression of the blending factor is stated in (20).

$$T_{axle} = (F_0 + F_1v + F_2v^2 + Ma) * r_{tire} \quad (19)$$

$$BF = \frac{Regen Tor}{Total Brake Tor} \quad (20)$$

For the drive cycle shown in Figure 21, all the points for the braking were pooled. Scatter plots of BF with respect to vehicle velocity and total braking torque were generated to observe the trends as shown in Figure 22.

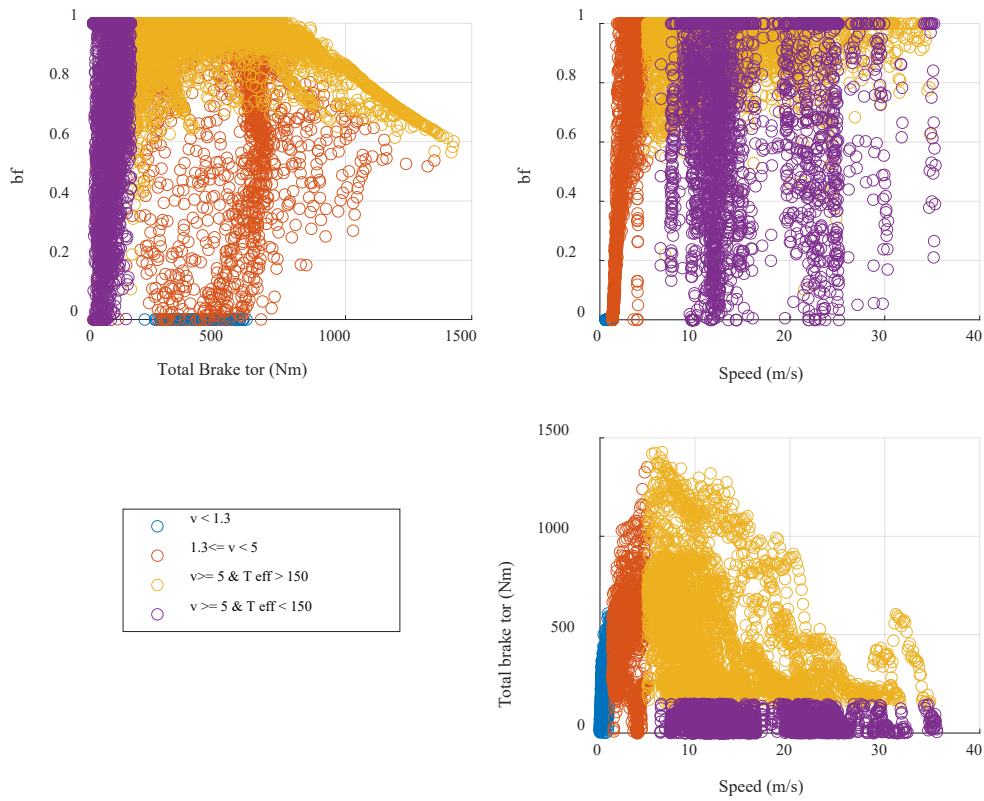


Figure 22 BF analysis

The following trends were observed from the scatter plots:

- 1) For speed less than 1.3 m/s, BF remains 0.

$$BF_{v < 1.3} = 0 \quad (21)$$

- 2) For speed between 1.3 m/s to 5 m/s, BF increased approximately linearly with the increase in vehicle speed from 0 to 1.

$$BF_{1.3 < v < 5.0} = 0.27 * v - 0.35 \quad (22)$$

- 3) For speed greater than 5 m/s, and total braking torque greater than 150 Nm, the BF remains maximum and is the function of the propulsion limits of the

vehicle. The regenerative braking torque limit of the motor is 860 Nm, as reflected from the data. So, for total brake torque less than 860 Nm, the BF is 1, but beyond the peak torque, the remaining torque is supplied by the friction brakes.

$$BF_{v>5.0,150<T<860} = 1 \quad (23)$$

$$BF_{v>5.0,T>860} = \frac{860}{\text{Total Brake Tor}} \quad (24)$$

- 4) For speed greater than 5m/s and total braking torque less than 150 Nm, the blending factor is approximated to be linearly increasing as the total brake torque request increases. A zoomed-in scatter plot is shown in Figure 23.

$$BF_{v>5.0,T<150} = \frac{T}{150} \quad (25)$$

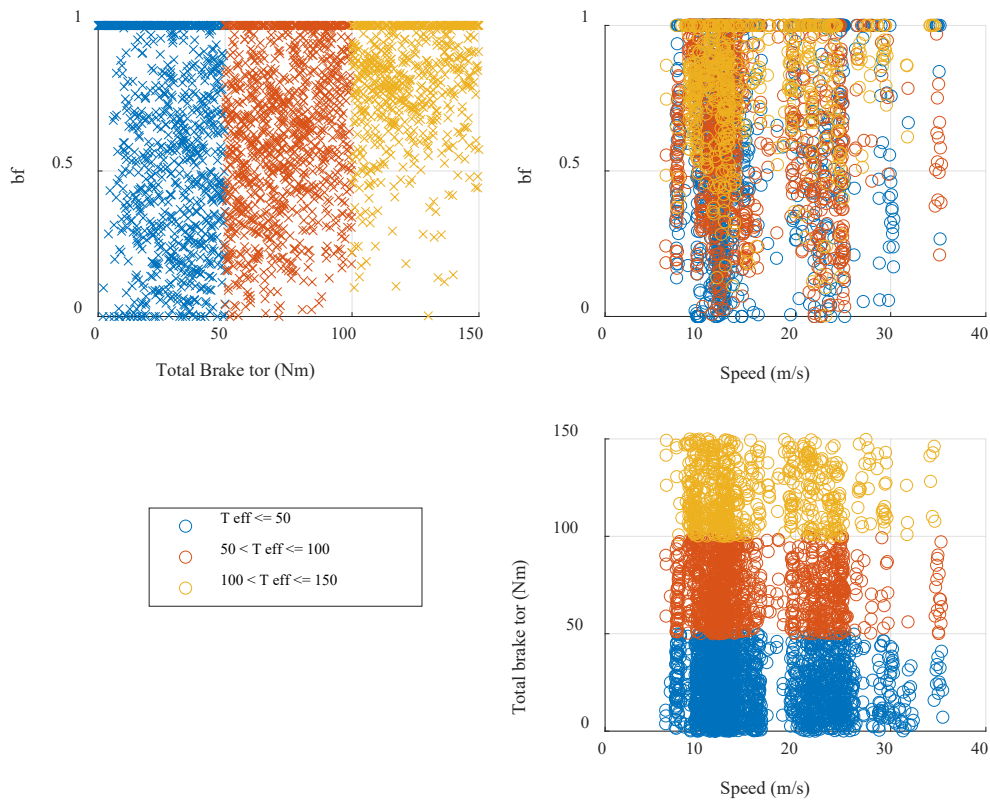


Figure 23 0-150 Nm total brake torque zoomed-in plot.

Determining the BF for the data has its challenges. Various factors affect the calculations and make it difficult to concretely estimate the critical values for blending strategy. Noise in the BF estimation can be observed in Figure 23, where the total brake torque is small. This noise can occur from factors like deviation in set coefficient, deviation in vehicle mass, and radius. Acceleration is estimated by taking the time derivative of the velocity and taking the derivative of discrete data can lead to increased noise.

Once the relation of BF with velocity and total brake torque is comprehended, it is coupled with the reduced-order energy model developed in section 4.3.1. By doing this, it is possible to bifurcate the total brake torque into its friction and regenerative braking components.

4.3.3 Developing Eco-AnD model for Bolt

The Eco-AnD model developed in section 4.1, can apply to any vehicle if a suitable cost function is provided. To extend the scope of the research, the Eco-AnD algorithm was developed for Bolt by using the reduced-order energy model developed in section 4.3.1 coupled with the blending strategy comprehended in section 4.3.2.

4.3.3.1 Cost function

The cost function to DP is developed using the reduced-order model developed for Bolt with a constant auxiliary load of 1.5 kW. The inputs to the reduced-order model are the vehicle velocity and the axle torque. The axle torque has only the regeneration portion of total brake torque as only it is responsible for harnessing energy back into the battery. The schematic for calculating the cost from the control input (acceleration) and state inputs (velocity, time) is similar as shown in Figure 13. By using the reduced-order energy model for the bolt the cost can be estimated for each iteration.

4.3.3.2 Constraints and inputs to DP

As explained in section 4.1, the constraints and inputs to the DP depend upon the road conditions and signal phase, and timing situation. The state inputs of velocity and time are the optimizer-generated values depending upon the minimum energy profile

possible. The constraint to maintain the speed limit is established using the MAP data from DSRC communication and another constraint of crossing the intersection during the green phase is established using the SPaT information. The distance from the intersection is calculated using the GPS in the vehicle and intersection coordinated broadcasted by the MAP messages.

4.3.4 Simulation Results for Bolt

The simulation result for the Eco-AnD algorithm developed for Bolt for the 6x6 intersection at ACM proving grounds. The results for intersection conditions as explained in Table 12 are shown in Figure 24. Subplot 2 shows the optimized speed profile for the intersection distance of 465 m. At -300m, the time remaining for the next green phase was 32 seconds, and subplot 2 shows the time taken to cross the intersection is just over 32 seconds. Subplot 3 shows the acceleration profile for the vehicle which remains within -1.4 m/s^2 to 0.7 m/s^2 . The energy consumption plot shows that the overall energy consumption for the maneuver is 226 kJ.

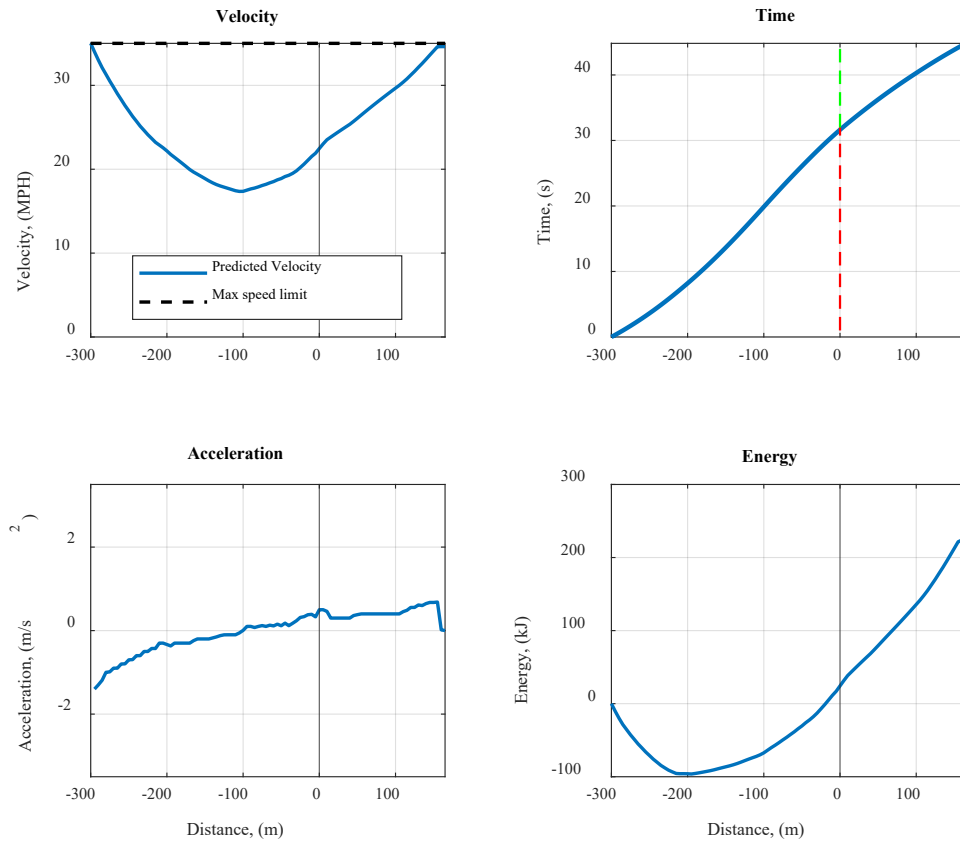


Figure 24 Simulation result for Bolt

The energy savings by the Eco-AnD algorithm is analyzed by comparing the speed profiles against the baseline case. Like Volt, the baseline speed profiles were developed for the bolt to mimic the human driver behaviors at intersections. For speed change maneuver constant acceleration and deceleration values of 1.45 m/s^2 were used as established in Table 13.

From Figure 25, the comparison of optimized speed profile and baseline speed profile can be seen. From subplot 2, it can be said that under both the case the vehicle takes

the almost same time to cover the distance of 465 m. Subplot 4 shows the comparison of the energy consumption. The energy consumed for the baseline case is 301 kJ and for the optimized speed profile, the energy consumption is 226 kJ, giving an energy saving of 25 % for the 6x6 intersection.

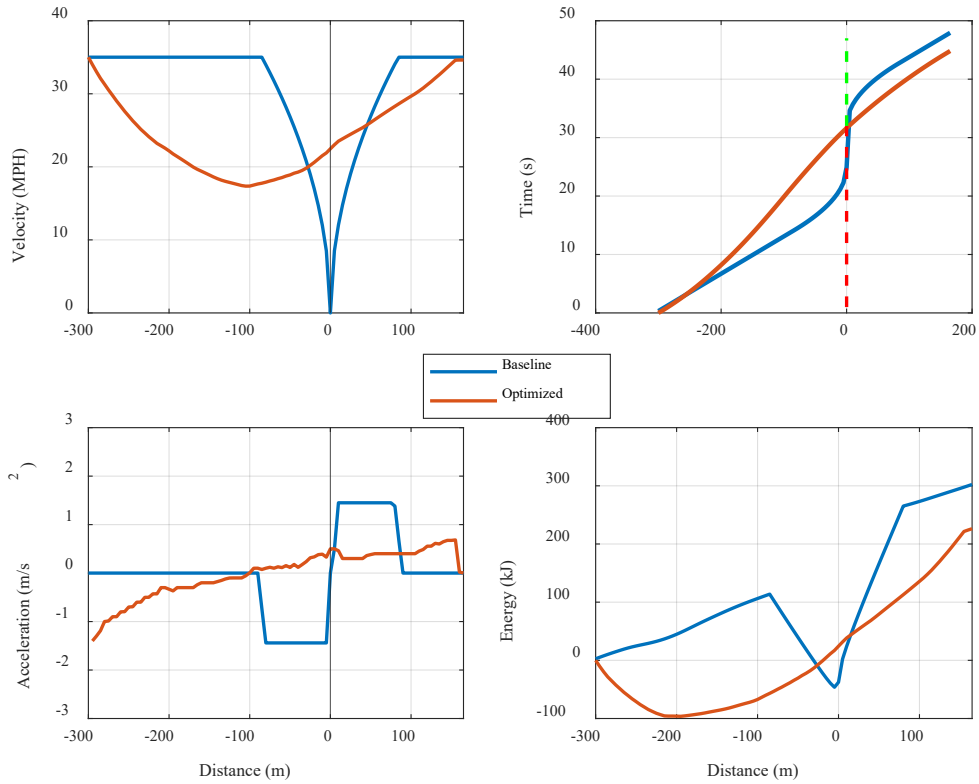


Figure 25 6x6 intersection baseline comparison - Bolt

5 Results and Discussions

Sections 4.1 & 4.3 described the Eco-AnD model development process for Volt and Bolt respectively. This section will focus on evaluating the energy-saving ability of the developed algorithm. The analysis is made both at simulation and vehicular level for Volt whereas for Bolt only simulation results are presented. But following the same procedures as for Volt, the estimates for energy benefits for Bolt can be made as well. This section also includes a discussion about the computation time of the dynamic programming algorithm. An analysis is shown in this section demonstrating the impact of discretization of states, control input, and problem length. It is also shown the effect of varied approach distance on energy savings and corresponding velocity profiles are shown. Lastly, the effect of vehicle mass on the optimized speed trajectory is discussed.

5.1 Eco-AnD energy benefits – Volt

5.1.1 Simulations

Simulation level energy benefits of the developed Eco-AnD model are made using the baseline model for Volt. An analysis is made for all the intersection crossings in the RSU loop and is also done for the intersections at ACM. As the result for the 6x6 intersection is shown in Figure 17, a similar analysis is made for all the intersections. The signal phase and timings measurements are used from the on-road/track testing observations and then replicated in the inputs for the DP as described in Table 12. The

intersections are designed in the simulations using observed road grades, speed limits, and intersection distances.

An elaborated description of simulated results for various intersections is shown in Table 19. The simulation cases described in that table are for the cases when a vehicle encounters a red phase as it enters the intersection. For a human driver without the knowledge of the signal timings, the baseline case is developed such that the vehicle comes to a rest at the intersection and waits for the phase to turn green. The optimizer with the knowledge of the signal phase and timings can generate the speed profiles that can avoid the complete stops and pass-through by slowing down the vehicle before reaching the intersection. The optimizer generated a velocity profile that reflects energy savings varying from 81 kJ to 108 kJ. Adding to the energy savings, a time-saving potential of the algorithm can also be observed.

Table 17 Eco-AnD simulated results for RSU loop intersections.

Property/Intersection	Lib. Int	DT Int.	Econo South	Walmart Int.	FF Int	Econo East Int.
Road grade (deg)	[-6.5, - 0.3]	[-1.5, 0.4]	[2.2, 3.0]	[2.3,2.6]	[1.0, 3.8]	[-4.2, 3.9]
Intersection distance (m)	600	600	600	600	600	600
Baseline Model Energy (kJ)	-84.5	304.4	953.4	915.1	634.9	324.6

Optimized Energy (kJ)	-165.6	219.3	844.7	806.2	532.2	233.1
Energy Saving (kJ)	81.1	85.1	108.6	108.8	102.7	91.5
Baseline Model Time (s)	59.1	63.4	55.2	54.9	62.9	57.2
Optimized Time (s)	56.2	59.8	54.0	53.9	59.6	54.8
Time saving (s)	2.9	3.6	1.2	1.0	3.3	2.4

Table 18 Eco-AnD simulated results for ACM intersections - Volt

Property/Intersection	6x6 Int	PMB Int
Road grade (deg)	[-0.4,1.1]	[-0.5, 0.6]
Intersection distance (m)	465	600
Baseline Model Energy (kJ)	382.1	431.3
Optimized Energy (kJ)	285.3	329.9
Energy Saving (kJ)	98.5	101.3
Baseline Model Time (s)	51	57.3
Optimized Time (s)	47.4	55.7
Time saving (s)	3.6	1.6

5.1.2 On-road Comparison

On-road comparisons of the energy consumption for Volt are made using MATLAB.

The cost function of the developed dynamic programming-based Eco-AnD algorithm

gives the energy consumption for the optimized speed profile. It takes the inputs of road grade and vehicle velocity to predict the energy consumption. The same energy model is also used to calculate the energy consumption for the on-road testing data collected around the MTU drive cycle and RSU loop by using the experimental speed and elevation profiles. Several tests run was made around the RSU loop while collecting the data to represent the energy consumption by a human driver at this corridor. For energy assessment at the simulation level first, the energy consumption by the human driver is compared against the optimized speed profile on an intersection basis. For six intersection crossings on the RSU loop data, the vehicle's energy consumption is calculated for the 600 m distance of each intersection using the vehicle's GPS.

For energy comparison vehicle's GPS data is used to extract the intersection start location 300 m away and intersection endpoint as well. Then the speed and grade vectors for the cut-out sections of each intersection are passed through a reduced-order energy model to calculate energy and then finally compare against the simulated speed profile. The optimized speed profile for each intersection is generated by considering the signal phase and timings.

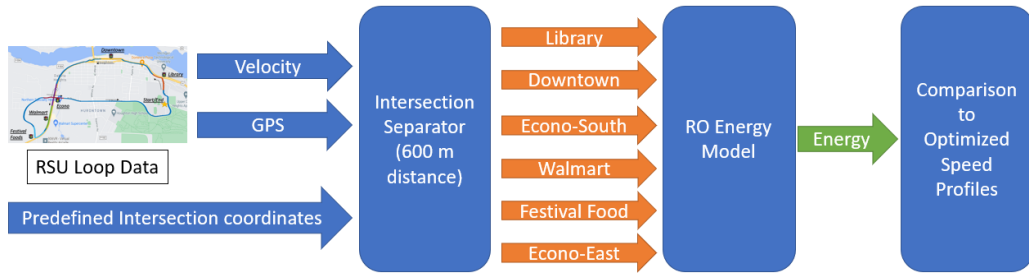


Figure 26 RSU loop simulation energy analysis

From a pool of 27 data sets, the energy analysis was carried out. From each of the data sets, the intersection with complete stops was considered and for those intersections, the energy-saving from optimized speed profile was recorded. Averaging out for all the available data sets these observed energy savings are laid out in Table 19.

Table 19 Eco-AnD on-road testing results for RSU loop.

Intersection	Energy – Data (kJ)	Energy – Optimized Speed profile (kJ)	Energy-saving (kJ)
Library	-100.0	-165.5	65.5
Downtown	278.8	219.3	59.5
Econo South	948.9	844.7	104.2
Walmart	944.8	806.2	138.6
Festival Foods	640.4	532.2	108.2
Econo East	288.7	233.1	55.6

One to one comparison on on-road test data and simulated speed profiles for intersections around the RSU loop shows that the energy savings per intersection vary from 55.6 kJ to 138.6 kJ depending upon the intersection.

This analysis is then extended to calculate the energy-saving potential for the RSU loop as well as for the MTU drive cycle. The process to estimate the energy saving is followed exactly as shown in Figure 26. The location-based energy estimate of human driving across the intersection is compared against the optimized speed profile's energy. The intersection with the complete vehicle stops allows estimating the energy savings as the optimizer generates the speed profiles such that the vehicle can cross the intersection without coming to a complete stop. Figure 27 shows the % energy savings for an RSU loop cycle with respect to the number of intersections with energy-saving potential.

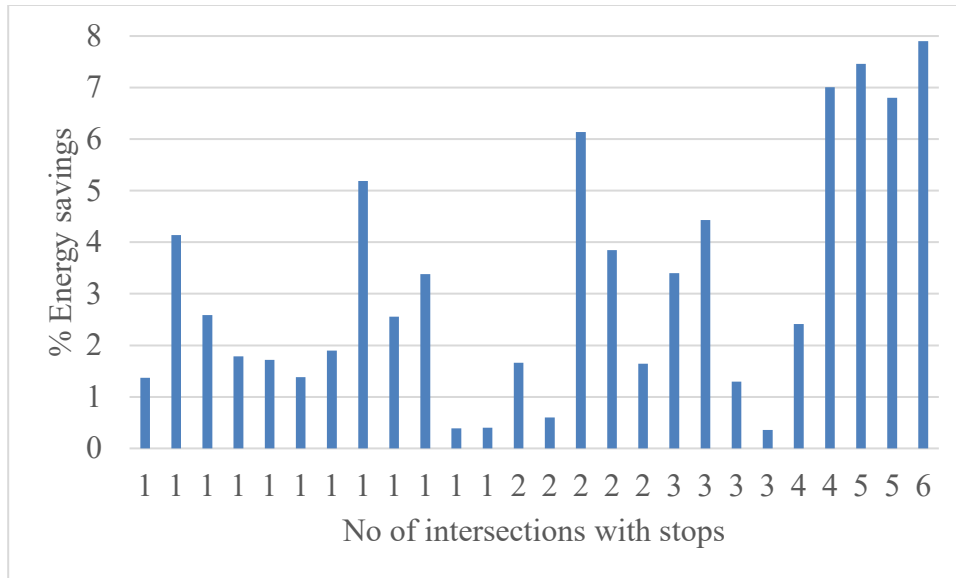


Figure 27 RSU loop energy savings with respect to the number of intersections with complete stops

It can be observed that the number of intersections with complete stops increases the energy savings potential of the algorithm increases. The maximum energy savings of 8% is observed when the optimizer avoids stopping at all six intersections. For data sets with one opportunistic intersection, the energy savings vary from 0.6 % to 5.1 %. This shows that the impact different signal phases and timings can make on the energy-saving potential around a corridor. The maximum energy savings are seen when the vehicle makes a complete stop at the intersection for the longer durations waiting for the green phase.

On similar lines, the analysis for the overall MTU drive cycle is carried out. From the 20 MTU drive cycle data sets available the energy-saving potential of the algorithm is computed. The results for the MTU drive cycle can be seen in Figure 28.

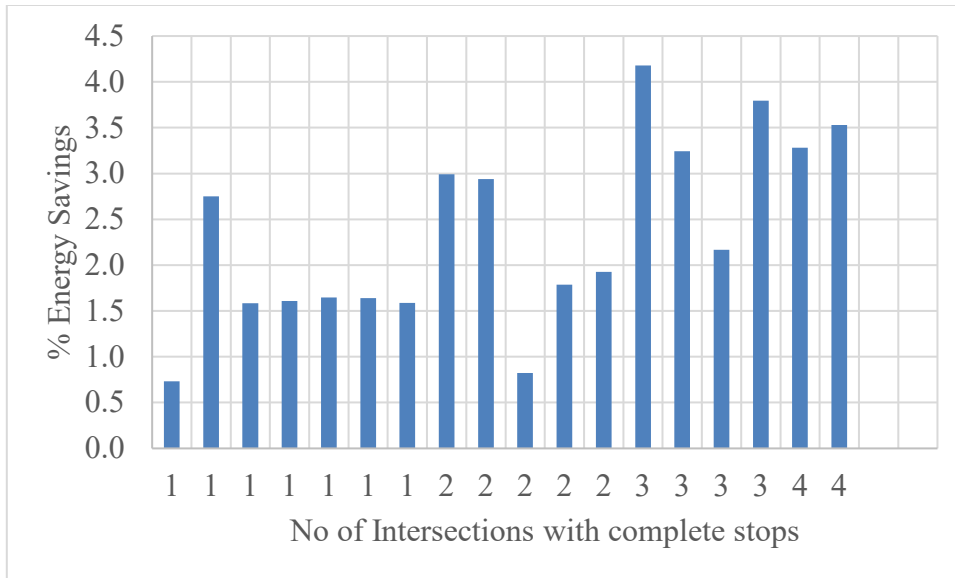


Figure 28 MTUDC Energy Savings vs Intersections with complete stops

It can be observed that the energy-saving potential varies from 0.7 % up to 4.2% for the overall MTU drive cycle. The energy savings depend upon the number of opportunistic intersections and phase timings of intersections. From the 20 data sets analyzed the maximum energy savings in observed for the drive cycle with 3 opportunistic intersections and a minimum energy saving is observed for the intersection with 1 opportunistic intersection.

5.1.3 Track testing

Sections 5.1.1 and 5.1.2 discuss the energy-saving potential of the developed algorithm in simulations and by using a hybrid approach where comparison is made between the energy consumption by on-road data and optimized speed profiles respectively. This section will discuss the track testing of the developed algorithm where experimental trials of the optimized speed profiles are made on actual vehicles and then energy

benefits are determined by analyzing the real-world experimental data vs human driver data. Track testing of the Eco-AnD algorithm was performed at ACM proving grounds and the intersection of focus is a 6x6 intersection. The intersection's comprehensive details can be found in Table 20.

Table 20 6x6 Intersection details

6x6 Intersection at ACM proving grounds	
Approach Distance (m)	300
Departure Distance (m)	165
Grade change	-2.1 to 2.4 deg
Speed limit	35 MPH
Green phase duration	25
Red phase duration	47
Yellow phase duration	4

To perform the track testing of the optimizer, the vehicle was made to follow the optimized speed profile using the drive-by-wire (DBW) system installed in the vehicle. The DBW system communicates with the MAB-II which provides the capability to control the vehicle in real-time. DBW system can control the various actuators in the vehicle such as the accelerator pedal, brake pedal, steering. To actuate various actuators with the DBW system, specific input commands can be given in real-time. DBW system comes with a speed control mode where the DBW system takes the input of speed command in m/s and then controls the accelerator pedal and brake pedals to

maintain the desired speed. Using the speed control mode of the DBW system it is possible to make the vehicle follow the location-based speed profile which otherwise would be difficult for a human driver to replicate without making errors.

For track testing of the Eco-AnD algorithm at ACM, the vehicle was made to follow the pre-defined optimized speed profile by giving the speed request command to the DBW system in speed control mode. The optimized speed profiles were generated beforehand for the signal phase and timing scenario described in Table 12. The scenario relates to a human driving case where the time to the next feasible green phase is 32 seconds and the current phase at the time of intersection entrance is red. Mapping the 6x6 intersection in simulations gives the optimized speed profile as shown in Figure 15, which is then given as the input to the DBW system. The various inputs to the DP and their source of information while performing track testing are described in Table 21.

Table 21 Source of inputs to DP for track testing

Inputs to DP	Source while track testing
Vehicle velocity	Vehicle CAN
Distance to intersection	MAP data and vehicle's GPS
Current Phase	Simulated
Time to next signal	Simulated
Speed limit	Simulated

The schematic for performing location-based speed control is shown in Figure 29. The designed algorithm takes the inputs from the vehicle's GPS of current vehicle location. The information of latitude, longitude, and elevation is then converted to Earth-centric-Earth fixed (ECEF) coordinate system for ease of calculations. Then a comparison is made between the vehicle's current location and a pre-defined map of the location and optimized speed generated by the Eco-AnD algorithm to find a point in the MAP nearest to the current location, called the reference point. Then the reference point is used to find the speed input for the DBW system from the optimized speed trajectory generated by the Eco-AnD algorithm. Giving the input of the optimized speed for the current location to the DBW system makes the vehicle follow the optimized speed trajectory and hence cross the intersection efficiently.

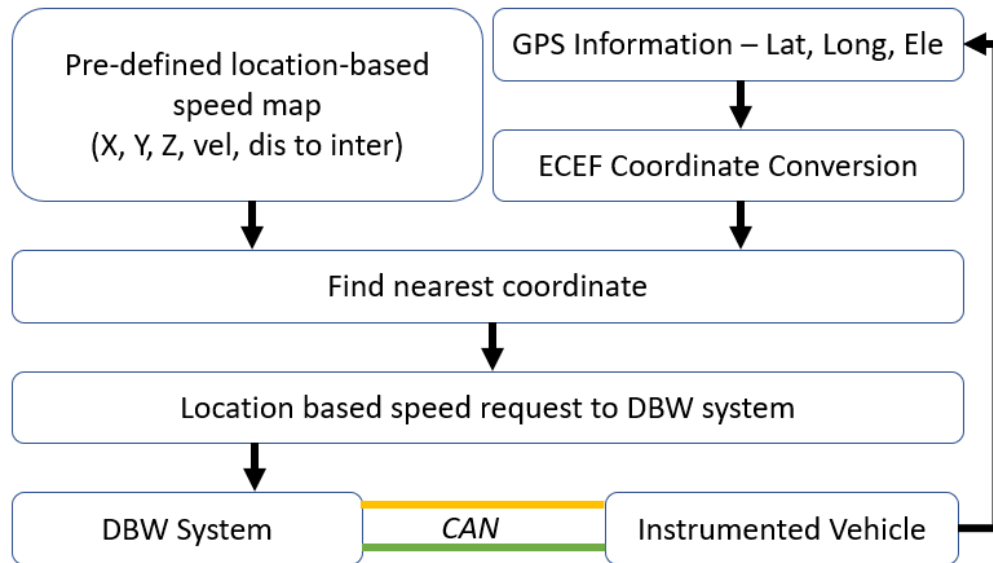


Figure 29 Location-based speed profile tracking.

The procedure for estimating the location-based speed request to the DBW system can further be explained as shown in Figure 30.

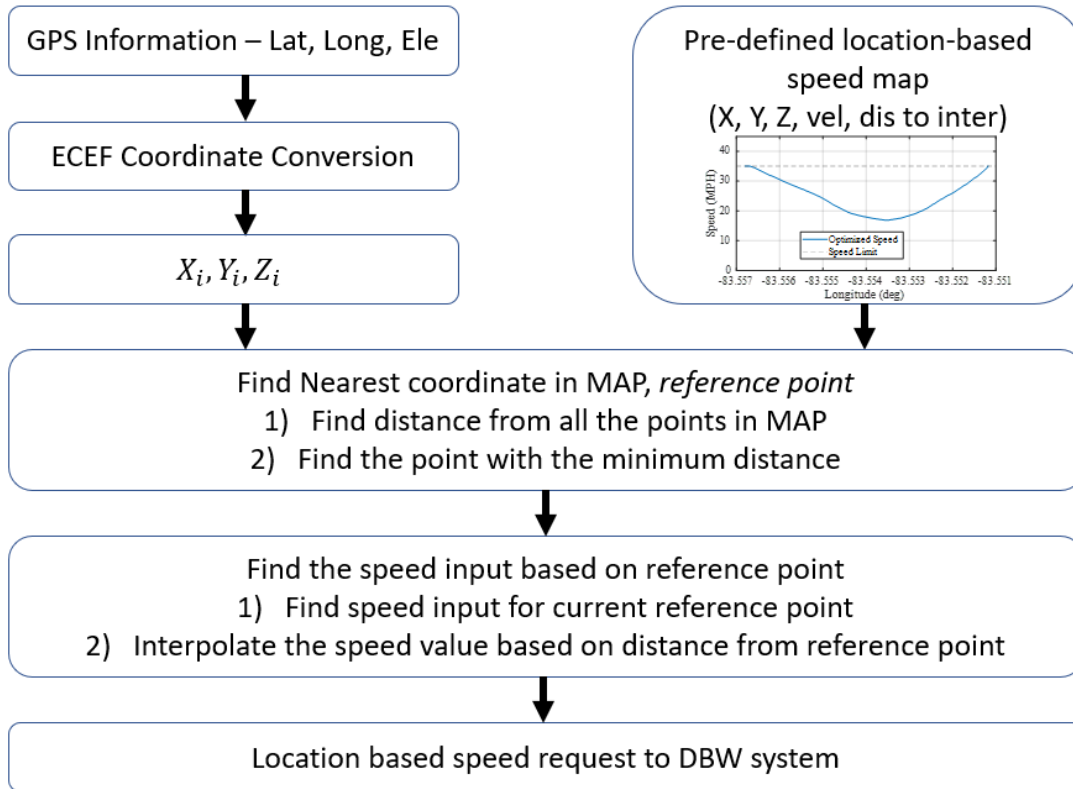


Figure 30 Schematic for determining speed request based on the reference point.

Track testing results for the 6x6 intersection can be visualized from Figure 31. Plots for comparison between human driving and optimized speed profile tracking are shown in four subplots. Subplot 1 shows the comparison of the vehicle speed for two cases where human-driven must come to a complete stop at the intersection (distance = 0), the vehicle under the control of optimal trajectory crossed the intersection without stopping. The speed of the vehicle shows down 200 m distance before the intersection to avoid the complete stop while is uneconomical from the energy standpoint. This is

validated from subplot 4 where the energy consumption of the human drive case can be seen to increase and surpass the optimal case after crossing the intersection. An overall energy benefit of 83.7 kJ is observed for this run.

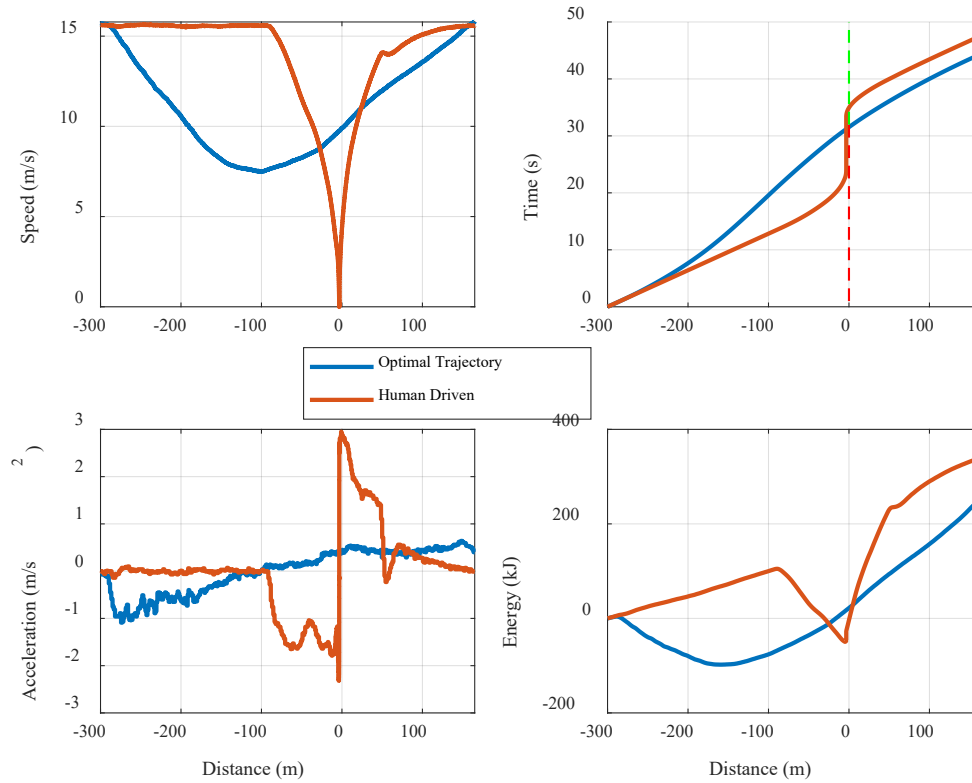


Figure 31 Track-testing result for 6x6 intersection

Following the comparison from subplot 2, it can be said that the optimized speed profile is not only energy efficient it is time-efficient too. A time benefit of 3.1 seconds can be observed at the end of the intersection (distance = 165 m). Subplot 3 shows the comparison of the vehicle acceleration and deceleration for both cases. The vehicle undergoes higher acceleration/decelerations in the human-driven case.

Repetitive testing for the above scenario was performed to check the repeatability testing of the energy savings by the Eco-AnD algorithm and account for the test-to-test variations. From Table 22 the average energy consumption for the human driver case is 360.3 kJ and that for location-based speed control is 256.3 kJ which gives an average energy savings of 104 kJ. Similarly, average time savings by the Eco-AnD algorithm is calculated to be 3.2 seconds for an intersection distance of 465 m.

Table 22 Track testing summary

Test Type	Energy Consumed (kJ)	Time for maneuver (s)
Human driven 1	368.5	47.5
Human driven 2	371.4	48.1
Human driven 3	340.9	47.7
Average Human driven	360.3	47.8
Speed Control 1	252.5	44.8
Speed Control 2	256.5	44.5
Speed Control 3	254.8	44.5
Speed Control 4	261.0	44.5
Average Speed Control	256.3	44.6

5.2 Eco-AnD energy benefits – Bolt

5.2.1 Simulations

The energy-saving potential of the dynamic programming base Eco-AnD algorithm for Bolt is discussed in detail in this section. The DP algorithm for Bolt is described in 4.3

and the baseline model development is described in 4.3.4. Detailed results for the potential energy savings by the Eco-AnD algorithm developed for Bolt are summarized in Table 23 & Table 24. First, the energy-saving potential around the RSU loop intersections is summarized. Energy-saving potential of 55 kJ to 95 kJ is observed depending upon the intersection. The time benefit for the algorithm is also summaries and varies from 0.3 seconds to 3.7 seconds. For the two intersections around ACM proving grounds, the energy benefits are about 75 kJ and time benefit of 3.1 seconds and 0.4 seconds for 6x6 and PMB intersection respectively.

Table 23 Eco-AnD results for RSU loop intersections - Bolt

Property Intersection	Lib.	DT	Econo South	Walmart	FF	Econo East
Road grade (deg)	[-6.5, - 0.3]	[-1.5, 0.4]	[2.2, 3.0]	[2.3,2.6]	[1.0, 3.8]	[-4.2, 3.9]
Intersection distance (m)	600	600	600	600	600	600
Baseline Model Energy (kJ)	-163.2	245.1	896.8	857.9	578.7	454.6
Optimized Energy (kJ)	-227.8	189.4	801.3	763.9	493.1	391.2
Energy Saving (kJ)	65.5	55.7	95.1	94.0	85.6	63.4
Baseline Model Time (s)	59.0	62.6	53.9	53.9	62.6	56.6

Optimized Time (s)	57.7	58.9	53.4	53.6	58.9	54.8
Time saving (s)	2.3	3.7	0.5	0.3	3.7	1.8

Table 24 Eco-AnD results for ACM intersections – Bolt

Property/Intersection	6x6 Int.	PMB Int.
Road grade (deg)	[-0.4,1.1]	[-0.5, 0.6]
Intersection distance (m)	465	600
Baseline Model Energy (kJ)	301.7	362.9
Optimized Energy (kJ)	226.3	284.0
Energy Saving (kJ)	75.4	78.9
Baseline Model Time (s)	47.9	56.6
Optimized Time (s)	44.8	56.2
Time saving (s)	3.1	0.4

5.2.2 On-road comparison

The energy-saving estimates for Bolt were made using the Bolt’s reduced order energy model. Following the similar estimation methodology as used in section 5.1.2 saving potential is estimated. From a data pool of 7 MTU drive cycles, the energy savings were estimated as shown in Figure 32.

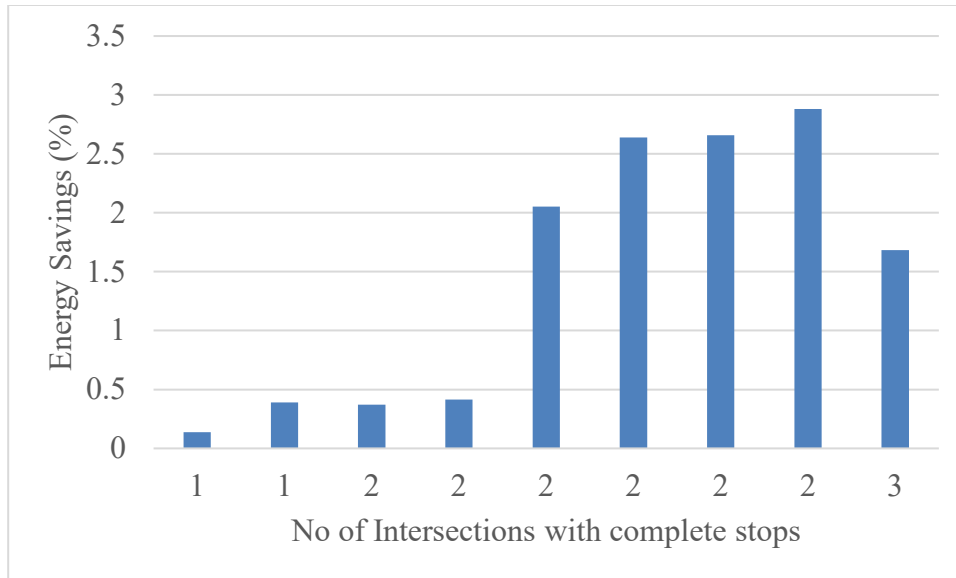


Figure 32 MTUDC Energy Savings vs Intersections with complete stops – Bolt

The maximum energy savings of 3 % is observed for a data set with two opportunistic intersections. For a data set with three intersections with complete stops, an energy saving of nearly 1.8 % is observed. A minimum energy saving of 0.2 % is shown for the data set with one intersection with a complete stop is observed.

5.2.3 Computation Time

For hardware implementation, the control logic must be computationally efficient such that when integrated into the real vehicle, the algorithm should be able to provide an optimized speed trajectory in the minimum possible time and with the available resources. A dynamic programming algorithm can be made computationally efficient by optimizing the grid discretization. For the problem in this research, there are two states (velocity and time), and one control input (acceleration). Iterating upon the different discretization of them Table 25 can be developed. These computation times

are based on a computer with a Core i7 processor and 16 GB of RAM. This table shows the energy savings (%) with each grid formation. The states and control inputs are discretizations in iterated and its effect on the energy savings is observed.

Table 25 Computation time for different grid discretization

Iteration No	Velocity Discretization (m/s)	Time Discretization (s)	Acceleration Discretization (m/s/s)	Energy Savings (%)	Computation Time (s)
1	0.20	0.10	0.10	-30.1	140.1
2	1.00	0.10	0.10	-30.1	28.8
3	1.00	0.20	0.10	-30.1	15.6
4	1.00	0.20	0.20	-30.0	7.8
5	1.00	0.10	0.20	-30.1	14.2
6	1.00	0.25	0.25	-29.9	5.4
7	1.50	0.25	0.25	-26.1	3.2
8	1.25	0.30	0.20	-29.6	4.4
9	1.50	0.50	0.30	-26.1	1.4

From the above nine iterations, the eighth iteration gives the best results as its computation time is around 4.4 seconds and the energy-saving potential is compromised by only 1.7 %. The computation time can be further brought down by reducing the limits of the states/control inputs. This iteration is shown in Table 26.

Table 26 Computation time for different control input limits

Iteration No	Acceleration min (m/s/s)	Acceleration max (m/s/s)	Acceleration Discretization (m/s/s)	Energy Savings (%)	Computation time (s)
1	-3.0	3.0	0.20	-30.0	7.8
2	-2.0	2.0	0.20	-30.0	5.9
3	-1.5	1.5	0.20	-29.2	3.5
4	-1.0	1.0	0.20	-29.3	2.6

From the table above, the best scenario is iteration 3 where the computation time is about 3.5 seconds. By following a similar procedure the computation time can be reduced further. Limiting the state grid and using the variable grid discretization type of methods can be used to make the algorithm computationally efficient. The overall problem of 600 m is discretized for every 5 m, giving 121 elements in total. The problem length can be discretized into a variable discrete level to make the algorithm even faster.

5.2.4 Variable Approach Distance

The approach distance for the problem is assumed to be 300 m for this research. The effect of different approach distances is studied and the corresponding energy-saving potential is noted. Table 27 summarizes the energy benefits corresponding to different

approach distances. The baseline energy for each case is calculated for a respective approach distance plus the 165 m of departure distance. It can be observed that even by reducing the approach distance by 50 m, the energy-saving potential on the algorithm is about 93.5 kJ, which is only 0.6 kJ less as compared to the case with 300 m approach distance.

Table 27 Effect of different approach distance

S.No	Approach Distance	Baseline Energy (kJ)	Optimized Energy (kJ)	Energy Savings (%)	Energy Difference (kJ)
1	300	352.8	258.7	-26.7	-94.1
2	280	342.7	249.0	-27.3	-93.7
3	270	337.8	244.2	-27.7	-93.6
4	260	333.1	239.4	-28.1	-93.7
5	250	328.2	234.7	-28.5	-93.5

The approach distance can vary because of the computation time required by the dynamic programming algorithm. If the algorithm takes 1 sec to compute the optimal trajectory, then the vehicle could cover a distance of 20.1 m, of moving at 45 MPH. Similarly, for different speeds the distance traveled while computing the optimized trajectory can be estimated and approach distance can be changed accordingly. The

various optimized speed profiles for the iterations from 300 m approach distance to 250 m of approach distance can be seen in Figure 33.

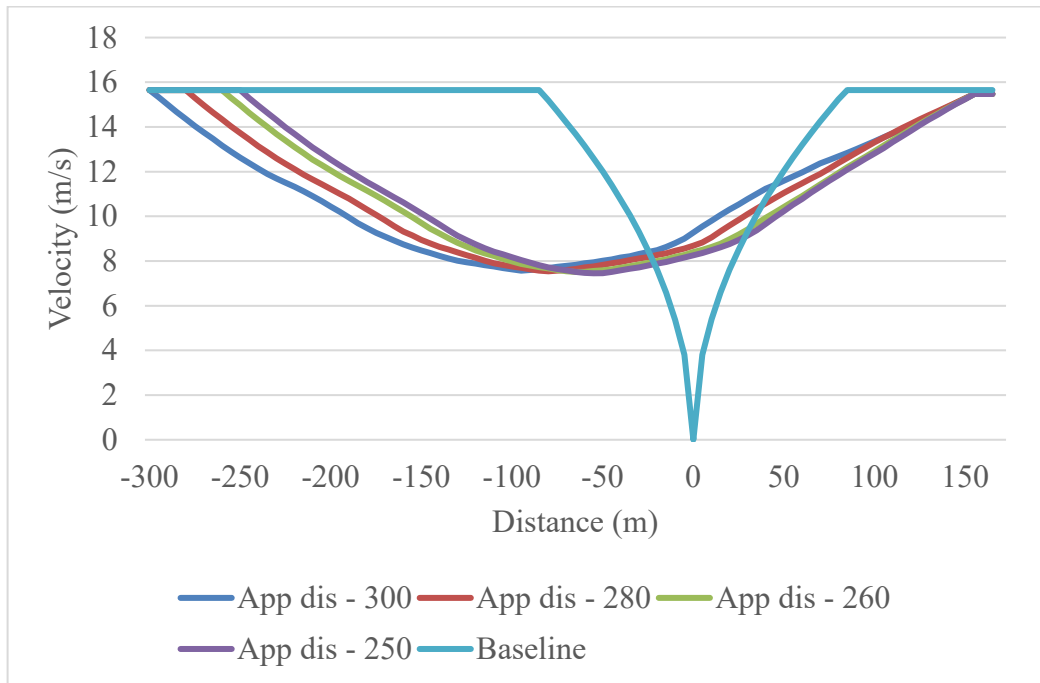


Figure 33 Iteration of different approach distance

5.2.5 Variable Vehicle Mass

Correct estimation of vehicle mass plays a very crucial role in determining the energy consumption for a vehicle. As the energy model developed in section 4.2 uses the vehicle mass as a parameter to determine the total axle torque using the vehicle's longitudinal dynamics equation. Given the complexity of correct estimation of vehicle mass total mass due to various factors such as the number of passengers, auxiliary load, etc, the effect of mass on the devised algorithm is studied. Table 28 describes the trends in energy savings on Volt, shown as %, with change in mass.

Table 28 Effect of different mass

S.No	Mass (as a factor of M)	Baseline Energy (kJ)	Optimized Energy (kJ)	Energy Savings (%)	Energy difference (kJ)
1	0.90xM	337.9	255.5	-24.4	-82.4
2	0.95xM	345.2	257.1	-25.5	-88.1
3	1.00xM	352.8	258.7	-26.7	-94.1
4	1.05xM	360.7	260.4	-27.8	-100.3
5	1.10xM	368.7	262.1	-28.9	-106.6

From the table above, the energy savings increase corresponds to the increase in mass of the vehicle. The optimized speed profiles for each of the iteration are shown in Figure 34. It can be observed that the optimized speed profiles for each iteration are close to each other and changing the mass even by 10 % did not have a significant impact on the optimized speed profile.

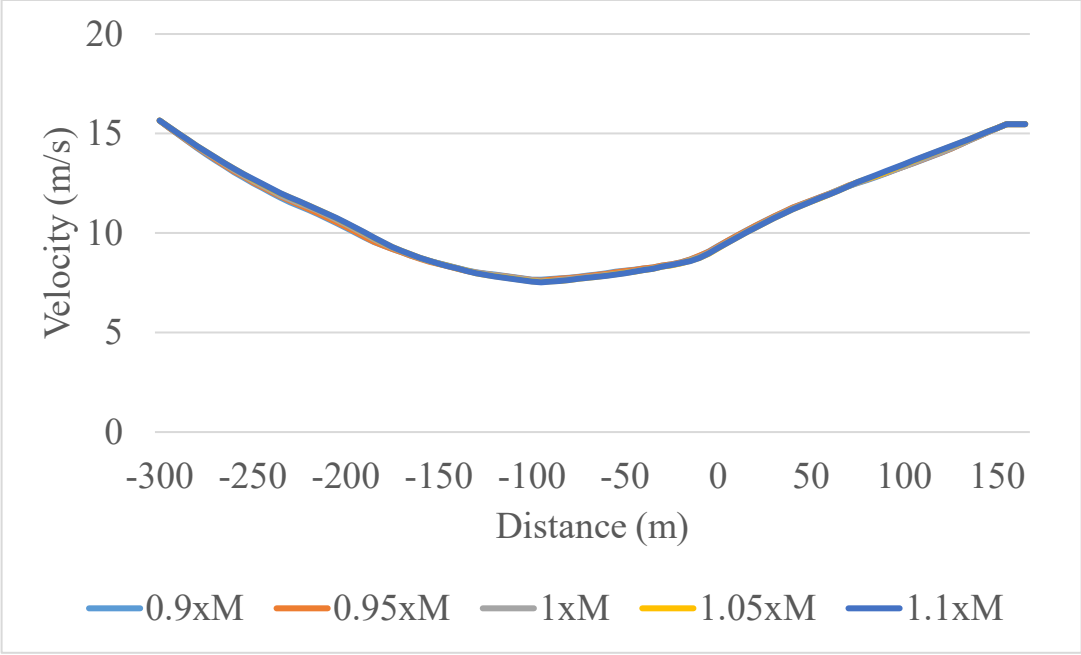


Figure 34 Iteration of different mass

6 Conclusions and future work

6.1 Conclusion

This study focused on extending upon an existing Eco-AnD algorithm from prior work at MTU. The algorithm was developed further by refining the input constraints to the dynamic programming for intersection crossing time making it possible for the algorithm to develop an optimized speed profile for all the possible scenarios of traffic phase state when the DSRC communication horizon of intersection is entered. The dynamic programming-based Eco-AnD algorithm developed in this study used the inputs from V2I communication for signal phase and timings, intersection, and road data. Using this information, the algorithm could generate an optimized speed profile capable to save both energy and time.

The devised algorithm was extended for Bolt to show that by only changing the cost function the algorithm can generate vehicle-specific velocity profiles. Bolt's reduced order energy model was developed by using the dynamometer data comprising of various standard and aggressive drive cycles. The vehicle's brake blending strategy was then modeled to add to the reduced-order energy model and then ultimately to be used in the cost function for the DP.

To show the energy savings results for simulation, on-road and track testing are presented. The algorithm was able to demonstrate energy savings in simulations, on-road test data, and track test data. Additional benefits of the algorithm could be seen as total travel time was reduced for crossing the intersection. For estimating the energy-

saving potential of the algorithm baseline speed profiles were developed and devised model was able to demonstrate a benefit of 55-95 kJ per intersection for Bolt and 81-108 kJ for Volt. On-road energy comparison was made for the RSU loop drive cycle to show an energy-saving potential of 0.5 to 8.0 % of energy for Volt depending upon the number of intersections with complete vehicle stops. A location-based speed profile tracking algorithm was devised and implemented to prove the energy savings by optimized speed profile. Track testing showed an energy savings of 104 kJ for the 6x6 intersection for GM-Volt and a time advantage of 3.2 seconds for the 6x6 intersection at ACM proving grounds.

6.2 Future Work

During this research, numerous challenges were faced. Many of those challenges were overcome such as developing the reduced-order energy model to be used as a cost function for GM Bolt. Still, there are quite a few horizons where the above research can be extended such as the real-time implementation of the algorithm, passenger comfort as a parameter for optimization, consideration of on-road traffic scenarios, uncertainty in the traffic phase timings, and extendability to other powertrain architectures.

The dynamic programming algorithm is a computationally demanding algorithm majorly due to the cost matrix calculation while backward progression. The computational need of the algorithm can be brought down significantly by making the state/control grid coarse. Heavy computation times need a faster processor for real-time

implementation which may not be a very cost-effective solution. So, finding an optimal state/control grid that meets the requirements for real-time implementation is necessary.

As we saw the optimized speed profile developed in section 5, the acceleration requested by the algorithm at -300 m changes from 0 to a certain value instantaneously. This maneuver when implemented on a real vehicle may not be very comfortable for the passenger as a sudden change in acceleration produces high jerks. This problem can be dealt with during the vehicle implementation phase where optimal speed profile is given as the input to the vehicle after smoothening using interpolation.

The current algorithm works on the assumption that the intersection is clear of other traffic, which may not be always the case. As the speed profile in section 5 slows down approximately 100 m before the intersection, this may cause disturbance in the preceding traffic. Another factor where the surrounding traffic plays an important role is when there is traffic waiting at the intersection for the green phase. This traffic pile-up will affect the optimized speed profile to cross the intersection safely.

Since the traffic light controllers at certain places are now equipped with much more advanced sensors to adjust the signal phase and time in real-time according to the traffic demand, so the Eco-AnD algorithm should also be robust enough to account for the uncertainty in the signal phase and timings.

7 Appendix

7.1 SPaT and MAP message directory

The table includes the details on the SPaT and MAP message directory that is used in section 4.1.

Table 29 V2I message directory

S.No.	Name	Message	Description
1	minEndTime	SPaT	Provides the information on the minimum time left for the next signal change
2	currentphase	SPaT	Provides the information on the current phase state 3 → Red 5 → Green 7 → Yellow
3	IntersectionID	MAP	Provides the ID of the intersection from which the message is being received
4	latitude	MAP	Provides the GPS latitude of the intersection
5	longitude	MAP	Provides the GPS longitude of the intersection
6	elevation	MAP	Provided the GPS elevation of the intersection

7.2 Computation Time

Table includes the several iteration performed on the computation time of algorithm as described in section 5.2.3.

Table 30 Computation time for different grid discretization (full table)

S.No	Velocity Discretization (m/s)	Time Discretization (s)	Acceleration Discretization (m/s/s)	Energy Saving (%)	Computation Time (s)
1	0.10	0.10	0.10	-25.70	261.10
2	0.20	0.10	0.10	-26.80	128.77
3	0.50	0.10	0.10	-25.90	53.57
4	0.75	0.10	0.10	-26.80	38.40
5	0.80	0.10	0.10	-28.50	35.01
6	1.00	0.10	0.10	-30.10	28.00
7	1.25	0.10	0.10	-29.90	25.58
8	1.50	0.10	0.10	-26.30	19.37
9	0.20	0.20	0.10	-26.70	67.70
10	0.20	0.30	0.10	-26.40	47.30
11	0.20	0.50	0.10	-26.60	29.57
12	0.20	0.75	0.10	-25.90	18.74
13	0.20	1.00	0.10	-25.70	14.48
14	0.20	1.25	0.10	-25.60	11.11
15	0.20	1.50	0.10	-25.50	9.12
16	0.20	2.00	0.10	-25.30	6.90
17	0.20	0.20	0.20	-26.60	34.20
18	0.20	0.20	0.30	-26.60	23.79
19	0.20	0.20	0.50	-26.40	15.56

Reference List

- [1] A. Islam, M. T. Hossan, and Y. M. Jang, "Convolutional Neural Network Scheme-Based Optical Camera Communication System for Intelligent Internet of Vehicles," *International Journal of Distributed Sensor Networks*, vol. 14, 02/07 2018, doi: 10.1177/1550147718770153.
- [2] ARPA-e. "Next-Generation Energy Technologies for Connected and Automated On-Road Vehicles." <https://arpa-e.energy.gov/technologies/programs/nextcar> (accessed 06/11/2021).
- [3] J. Oncken *et al.*, "A Connected Controls and Optimization System for Vehicle Dynamics and Powertrain Operation on a Light-Duty Plug-In Multi-Mode Hybrid Electric Vehicle," 2020. [Online]. Available: <https://doi.org/10.4271/2020-01-0591>.
- [4] B. Narodzonek, J. Naber, D. Robinette, and J. Worm, "DEVELOPMENT OF AN ECO APPROACH AND DEPARTURE APPLICATION TO IMPROVE ENERGY CONSUMPTION OF A PLUG-IN HYBRID VEHICLE IN CHARGE DEPLETING MODE," Michigan Technological University, Houghton, Michigan, 2020.
- [5] P. Emami, M. Pourmehr, M. Martin-Gasulla, S. Ranka, and L. Elefteriadou, "A Comparison of Intelligent Signalized Intersection Controllers Under Mixed Traffic," in *2018 21st International Conference on Intelligent Transportation Systems (ITSC)*, 4-7 Nov. 2018 2018, pp. 341-348, doi: 10.1109/ITSC.2018.8569939.

- [6] *Dedicated Short Range Communications (DSRC) Message Set Dictionary*, V. X. C. T. Committee, 2016. [Online]. Available: https://doi.org/10.4271/J2735_201603
- [7] B. Asadi and A. Vahidi, "Predictive Use of Traffic Signal State for Fuel Saving," *IFAC Proceedings Volumes*, vol. 42, no. 15, pp. 484-489, 2009/01/01/2009, doi: <https://doi.org/10.3182/20090902-3-US-2007.0064>.
- [8] U. Vögele and C. Endisch, "Predictive Vehicle Velocity Control using Dynamic Traffic Information," 2016. [Online]. Available: <https://doi.org/10.4271/2016-01-0121>.
- [9] L. Guo, B. Gao, Y. Gao, and H. Chen, "Optimal Energy Management for HEVs in Eco-Driving Applications Using Bi-Level MPC," *IEEE Transactions on Intelligent Transportation Systems*, vol. 18, no. 8, pp. 2153-2162, 2017, doi: 10.1109/TITS.2016.2634019.
- [10] P. Hao, G. Wu, K. Boriboonsomsin, and M. J. Barth, "Eco-Approach and Departure (EAD) Application for Actuated Signals in Real-World Traffic," *IEEE Transactions on Intelligent Transportation Systems*, vol. 20, no. 1, pp. 30-40, 2019, doi: 10.1109/TITS.2018.2794509.
- [11] M. R. Cantas, O. Kavas, S. Tamilarasan, S. Y. Gelbal, and L. Guvenc, "Use of Hardware in the Loop (HIL) Simulation for Developing Connected Autonomous Vehicle (CAV) Applications," 2019. [Online]. Available: <https://doi.org/10.4271/2019-01-1063>.

- [12] C. Sun, J. Guanetti, F. Borrelli, and S. J. Moura, "Optimal Eco-Driving Control of Connected and Autonomous Vehicles Through Signalized Intersections," *IEEE Internet of Things Journal*, vol. 7, no. 5, pp. 3759-3773, 2020, doi: 10.1109/JIOT.2020.2968120.
- [13] B. Barik, B. Chen, M. Shahbakhti, and D. L. Robinette, "Designing a Real-time Velocity Predictor for Powertrain Optimization of Connected and Automated Vehicles," Michigan Technological University, Houghton, Michigan, 2017.
- [14] N. Rama and D. Robinette, "Computationally Efficient Reduced-Order Powertrain Model of a Multi-Mode Plug-In Hybrid Electric Vehicle for Connected and Automated Vehicles," 2019. [Online]. Available: <https://doi.org/10.4271/2019-01-1210>.
- [15] Chevrolet. "Chevrolet Volt - 2016." <https://media.chevrolet.com/media/us/en/chevrolet/vehicles/volt/2016.tab1.html> (accessed 6/11/2021).
- [16] Chevrolet. "Chevrolet Bolt Ev - 2019." <https://media.chevrolet.com/media/us/en/chevrolet/vehicles/bolt-ev/2019.tab1.html> (accessed 6/11/2021).
- [17] D. Robinette *et al.*, "PHEV Real World Driving Cycle Energy and Fuel and Consumption Reduction Potential for Connected and Automated Vehicles," 2019. [Online]. Available: <https://doi.org/10.4271/2019-01-0307>.

- [18] O. Sundstrom and L. Guzzella, "A generic dynamic programming Matlab function," in *2009 IEEE Control Applications, (CCA) & Intelligent Control, (ISIC)*, 8-10 July 2009 2009, pp. 1625-1630, doi: 10.1109/CCA.2009.5281131.
- [19] J. Wang, K. K. Dixon, H. Li, and J. Ogle, "Normal Acceleration Behavior of Passenger Vehicles Starting from Rest at All-Way Stop-Controlled Intersections," *Transportation Research Record*, vol. 1883, no. 1, pp. 158-166, 2004, doi: 10.3141/1883-18.
- [20] J. Wang, K. Dixon, H. Li, and J. Ogle, "Normal Deceleration Behavior of Passenger Vehicles at Stop Sign–Controlled Intersections Evaluated with In-Vehicle Global Positioning System Data," *Transportation Research Record: Journal of the Transportation Research Board*, vol. 1937, pp. 120-127, 01/01 2005, doi: 10.1177/0361198105193700117.
- [21] U. S. E. P. Agency. "Vehicle and Fuel Emissions Testing." <https://www.epa.gov/vehicle-and-fuel-emissions-testing/dynamometer-drive-schedules> (accessed 6/11/2021).
- [22] F. Momen, K. Rahman, Y. Son, and P. Savagian, "Electrical propulsion system design of Chevrolet Bolt battery electric vehicle," in *2016 IEEE Energy Conversion Congress and Exposition (ECCE)*, 18-22 Sept. 2016 2016, pp. 1-8, doi: 10.1109/ECCE.2016.7855076.
- [23] U. S. E. P. Agency. "Data on Cars used for Testing Fuel Economy." <https://www.epa.gov/compliance-and-fuel-economy-data/data-cars-used-testing-fuel-economy> (accessed 6/11/2021).